

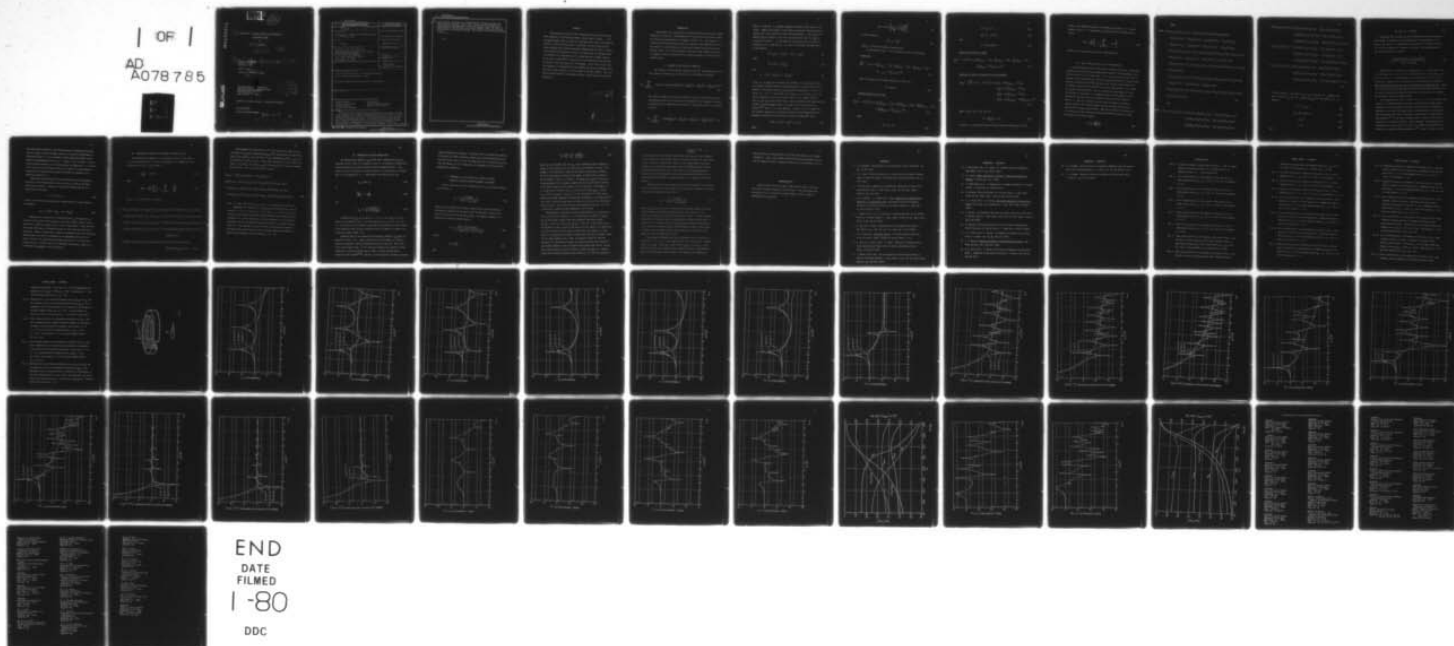
AD-A078 785

PENNSYLVANIA STATE UNIV UNIVERSITY PARK APPLIED RESE--ETC F/G 20/11  
VIBRATION OF A CLAMPED CIRCULAR PLATE DRIVEN BY A NONCENTRAL FO--ETC(U)  
OCT 79 J C SNOWDON  
N00024-79-C-6043  
NL

UNCLASSIFIED

1 OF 1

AD  
A078 785



ADA 078785

LEVEL

(92)

(6) VIBRATION OF A CLAMPED CIRCULAR PLATE DRIVEN BY  
A NONCENTRAL FORCE ,

by

(10) J. C. / Snowdon

(11) 31 Oct 79

(12) 57

(9) Technical Memorandum  
File No. 79-191  
October 31, 1979

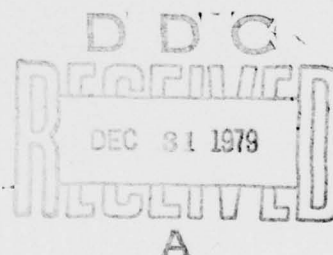
(14) ARL/PSU/TM-79-191

Copy No. 46

Contract No. N00024-79-C-6043

(15)

The Pennsylvania State University  
Institute for Science and Engineering  
APPLIED RESEARCH LABORATORY  
Post Office Box 30  
State College, PA 16801



Approved for public release: distribution unlimited

NAVY DEPARTMENT

NAVAL SEA SYSTEMS COMMAND

391 007

LB

79 12 31 027

DDC FILE COPY

UNCLASSIFIED

SECURITY CLASSIFICATION OF THIS PAGE (When Data Entered)

REPORT DOCUMENTATION PAGE		READ INSTRUCTIONS BEFORE COMPLETING FORM
1. REPORT NUMBER TM 79-191	2. GOVT ACCESSION NO.	3. RECIPIENT'S CATALOG NUMBER
4. TITLE (and Subtitle)  Vibration of a Clamped Circular Plate Driven by a Noncentral Force		5. TYPE OF REPORT & PERIOD COVERED
		6. PERFORMING ORG. REPORT NUMBER
7. AUTHOR(s)  J. C. Snowdon		8. CONTRACT OR GRANT NUMBER(s)  N00024-79-C-6043
9. PERFORMING ORGANIZATION NAME AND ADDRESS  The Pennsylvania State University Applied Research Laboratory, P. O. Box 30, State College, PA 16801		10. PROGRAM ELEMENT, PROJECT, TASK AREA & WORK UNIT NUMBERS
11. CONTROLLING OFFICE NAME AND ADDRESS U. S. Naval Sea Systems Command Department of the Navy Washington, DC 20362		12. REPORT DATE October 31, 1979
		13. NUMBER OF PAGES 57
14. MONITORING AGENCY NAME & ADDRESS (if different from Controlling Office)		15. SECURITY CLASS. (of this report)  UNCLASSIFIED
		15a. DECLASSIFICATION/DOWNGRADING SCHEDULE
16. DISTRIBUTION STATEMENT (of this Report)  Approved for public release; distribution unlimited. (As per letter dated December 3, 1979.)		
17. DISTRIBUTION STATEMENT (of the abstract entered in Block 20, if different from Report)		
18. SUPPLEMENTARY NOTES		
19. KEY WORDS (Continue on reverse side if necessary and identify by block number)  Transmissibility.                      Mass loading. Clamped circular plate.              Dynamic vibration absorber. Internal damping.                      Arbitrary driving point. Driving-point impedance.		
20. ABSTRACT (Continue on reverse side if necessary and identify by block number)  Expressions are stated for the transmissibility and for the driving-point impedance of an internally damped circular plate of radius $a$ with a clamped boundary that is driven by a vibratory point force at an arbitrary distance $\rho_a$ from the plate center. Expressions are also stated for the plate transmissibility when the plate is loaded at the arbitrary driving point either by a lumped mass, by a dynamic vibration absorber--or, simultaneously, by a lumped mass and a dynamic absorber. In all cases, <span style="float: right;">not long</span>		

UNCLASSIFIED

SECURITY CLASSIFICATION OF THIS PAGE(When Data Entered)

→ representative calculations of transmissibility are plotted versus the square root of frequency. These curves clearly show the dependence of transmissibility and impedance on the plate damping factor, the value of the parameter  $\mu$ , and the extent of the mass loading. They also show the effectiveness of the dynamic absorber, which varies with the value assigned to  $\mu$ .

$\mu$

UNCLASSIFIED

SECURITY CLASSIFICATION OF THIS PAGE(When Data Entered)



## ABSTRACT

Expressions are stated for the transmissibility and for the driving-point impedance of an internally damped circular plate of radius  $a$  with a clamped boundary that is driven by a vibratory point force at an arbitrary distance  $\mu a$  from the plate center. Expressions are also stated for the plate transmissibility and driving-point impedance when the plate is loaded at the arbitrary driving point either by a lumped mass, by a dynamic vibration absorber--or, simultaneously by a lumped mass and a dynamic absorber. In all cases, representative calculations of transmissibility and impedance are plotted versus the square root of frequency. These curves clearly show the dependence of transmissibility and impedance on the plate damping factor, the value of the parameter  $\mu$ , and the extent of the mass loading. They also show the effectiveness of the dynamic absorber, which varies with the value assigned to  $\mu$ .

Accession For	
NTIS GRA&I	<input checked="" type="checkbox"/>
DDC TAB	<input type="checkbox"/>
Unannounced	<input type="checkbox"/>
Justification	
By	
Distribution/	
Availability Codes	
Disc	Avail and/or special
<input checked="" type="checkbox"/>	<input type="checkbox"/>

## INTRODUCTION

The response of circular plates to noncentral forces has not been studied extensively in the past. The deformation of circular plates statically loaded off center has been discussed, for example, in Refs. 1-11. The response of a circular plate when transiently loaded off center has been addressed in Ref. 12. The response of circular plates to noncentral vibratory forces has been considered in Refs. 13-17, which represent a relatively small number of articles as compared to those concerned with the vibration response of centrally driven circular plates.

## I. SOLUTION TO THE THIN-PLATE EQUATION

The solution to the thin-plate equation yields the following equation for the transverse deflection  $\tilde{\xi}_k$  of the plate in its  $k$ th mode of vibration:

$$\tilde{\xi}_k = \sum_{k=0,1,2,\dots} (A_k \cos k\theta + B_k \sin k\theta) [P_k^* J_k(n^* r) + Q_k^* Y_k(n^* r) + R_k^* I_k(n^* r) + S_k^* K_k(n^* r)] e^{j\omega t}, \quad (1)$$

and, when the origin of the polar coordinates is taken as the radial line passing through the point of excitation of the noncentral force (because a solution is required that is symmetrical with respect to this radial line) it is possible to write

$$\tilde{\xi}_k = \sum_{k=0,1,2,\dots} \cos k\theta [P_k^* J_k(n^* r) + Q_k^* Y_k(n^* r) + R_k^* I_k(n^* r) + S_k^* K_k(n^* r)] e^{j\omega t}. \quad (2)$$

Here,  $t$  is time and  $\omega$  is angular frequency, hereafter known simply as frequency. Symbols with superior tildes denote sinusoidally varying quantities, symbols with a star superscript denote complex quantities. The ordinary and modified Bessel functions of the first and second kinds have the complex argument  $(n^* r)$  where  $r$  is the radius of the arbitrary point to which the noncentral force is applied (Fig. 1), and  $n^*$  is the plate wavenumber given by the equation

$$n^* = n\{[1 - (v^*)^2]/(1 - v^2)(1 + j\delta_{E\omega})\}^{1/4}, \quad (3)$$

where

$$n^4 = \omega^2 \rho (1 - v^2) / r_g^2 E_\omega \quad (4)$$

and

$$[1 - (v^*)^2] = (E_\omega^* / G_\omega^*) [1 - (E_\omega^* / 4G_\omega^*)] \quad (5)$$

In Eq. (1),  $A_k$  and  $B_k$  are arbitrary real constants, and  $P_k^*$ ,  $Q_k^*$ ,  $R_k^*$ , and  $S_k^*$  are arbitrary complex constants, where  $Q_k^*$  and  $S_k^*$  are zero for a plate that is complete to the center because  $Y_k$  and  $K_k$  exhibit singularities as  $(n^* r) \rightarrow 0$ . In Eqs. (3) - (5),  $\rho$  is the density of the plate,  $a$  is its radius,  $r_g$  is the radius of gyration of its cross section, and  $v^*$  is its complex Poisson's ratio;  $E_\omega^*$  and  $G_\omega^*$  are the complex Young's and shear moduli of the plate material. If their associated damping factors are equal, as can realistically be assumed,<sup>18,19</sup> then  $v^* = v$ , a real quantity. Further, if it is assumed that the frequency dependence of  $E_\omega^*$  and  $G_\omega^*$  and their associated damping factors is negligible (damping of the solid type or hysteretic damping<sup>18</sup>), then

$$(n^* a) = (na)/(1 + j\delta_E)^{1/4} = (p + jq) \quad (6)$$

where

$$p, q = \pm (na) \left[ \frac{1}{2 \sqrt{D_E}} \pm \frac{(1 + D_E)^{1/2}}{2 \sqrt{2} D_E} \right] ; \quad (7)$$

in this equation,

$$D_E = (1 + \delta_E^2)^{1/2} , \quad (8)$$

where  $\delta_E$  is the Young's modulus damping factor.

For the mode of order  $k$  it is possible to write the following:

#### Plate Slope

$$\begin{aligned} \frac{\partial \tilde{\xi}_k}{\partial r} = & - n^* \cos k\theta \{ P_k^* [J_{(k+1)}^* - T^* J_k^*] + Q_k^* [Y_{(k+1)}^* - T^* Y_k^*] - R_k^* [I_{(k+1)}^* + T^* I_k^*] \\ & + S_k^* [K_{(k+1)}^* - T^* K_k^*] \} (n^* r) e^{j\omega t} , \end{aligned} \quad (9)$$

where the argument of the Bessel functions is  $(n^* r)$ , and

$$T^* = k / (n^* r) . \quad (10)$$

#### Bending Moment/Unit Arc Length

$$\begin{aligned} B_k(r) = & - D^* (n^*)^2 \cos k\theta \{ P_k^* [\phi_r^* J_{(k+1)}^* - \alpha^* J_k^*] + Q_k^* [\phi_r^* Y_{(k+1)}^* - \alpha^* Y_k^*] - R_k^* [\phi_r^* I_{(k+1)}^* - \varepsilon^* I_k^*] \\ & + S_R^* [\phi_r^* K_{(k+1)}^* + \varepsilon^* K_k^*] \} (n^* r) e^{j\omega t} , \end{aligned} \quad (11)$$

where

$$\alpha^* = (1 - \Gamma^*) , \quad (12)$$

$$\epsilon^* = (1 + \Gamma^*) \quad , \quad (13)$$

$$\phi_r^* = (1 - \nu)/(n^* r) \quad , \quad (14)$$

and

$$\Gamma^* = k(k-1)\phi_r^*/(n^* r) \quad . \quad (15)$$

#### Shearing Force/Unit Arc Length

$$\begin{aligned} \tilde{F}_k(r) = & - D^* (n^*)^3 \cos k\theta \{ P_k^* [J_{(k+1)} - T^* J_k] + Q_k^* [Y_{(k+1)} - T^* Y_k] + R_k^* [I_{(k+1)} + T^* I_k] \\ & - S_k^* [K_{(k+1)} - T^* K_k] \} (n^* r) e^{j\omega t} \quad . \end{aligned} \quad (16)$$

#### Shearing Force/Unit Arc Length at the Plate Boundary

$$\begin{aligned} [\tilde{F}_k(r) - \frac{1}{r} \frac{\partial B_k}{\partial r} (r, \theta)] = & - D^* (n^*)^3 \cos k\theta \{ P_k^* [(1 + kT^* \phi_r^*) J_{(k+1)} - T^* \epsilon^* J_k] \\ & + Q_k^* [(1 + kT^* \phi_r^*) Y_{(k+1)} - T^* \epsilon^* Y_k] \\ & + R_k^* [(1 - kT^* \phi_r^*) I_{(k+1)} + T^* \alpha^* I_k] \\ & - S_k^* [(1 - kT^* \phi_r^*) K_{(k+1)} - T^* \alpha^* K_k] \} (n^* r) e^{j\omega t} \quad , \end{aligned} \quad (17)$$

where, in Eqs. (11), (16), and (17),

$$D^* = dE_\omega r_g^2 / (1 - \nu^2) \quad (18)$$

in which  $d$  is the plate thickness and the radius of gyration  $r_g = d/2\sqrt{3}$ .



Finally, the impressed force/unit arc length at the radius  $r = b = \mu a$  and angular location  $\theta$  is conveniently represented by the following Fourier series:

$$\tilde{F}(\theta) = \frac{\tilde{F}_0}{2\pi b} \left[ 1 + 2 \sum_{k=1,2,3,\dots}^{\infty} \cos k\theta \right], \quad (19)$$

where  $\tilde{F}_0$  is the concentrated (discrete) impressed force.

## II. Force Transmissibility to the Plate Boundary

By considering the plate as two plates--a central plate plus a surrounding annular plate--that are joined together with continuity of displacement, slope, and bending moment at the same radius  $r = b = \mu a$  as that to which the force is applied, and by considering the sum of the shearing force/unit arc length around the outer perimeter of the inner circular plate, and the shearing force/unit arc length around the inner perimeter of the outer annular plate, to be equal to the force specified by Eq. (19), by equating the displacement and slope of the plate to zero where it is clamped around its outer boundary, and by writing down the force that is transmitted to the outer plate boundary where  $r = a$ , then it is possible to write down six equations for the six complex constants for the entire plate (two for the inner circular plate and four for the outer annular plate). When these equations are solved for, it is possible to write down the following expression for the force transmissibility to the plate boundary:

$$T = \frac{1}{\mu} \left| \frac{(\text{NUM.})}{(\text{DEN.})} \right|, \quad (20)$$

where

$$\begin{aligned}
 (\text{NUM.}) = & \{[(J_{1\mu} - T_{\mu} J_{o\mu})(\phi_{\mu} I_{1\mu} - \epsilon I_{o\mu}) - (\phi_{\mu} J_{1\mu} - \alpha J_{o\mu})(I_{1\mu} + T_{\mu} I_{o\mu})][J_1 Y_{o\mu}(I_o K_1 + K_o I_1) \\
 & - J_1 K_{o\mu}(Y_o I_1 + Y_1 I_o) + Y_1 K_{o\mu}(J_o I_1 + J_1 I_o) + I_1 J_{o\mu}(Y_o K_1 - Y_1 K_o) - I_1 Y_{o\mu}(J_o K_1 - J_1 K_o) \\
 & + I_1 K_{o\mu}(J_o Y_1 - J_1 Y_o) + I_1 K_o J_{o\mu}(Y_1 - T Y_o) + K_1 Y_{o\mu}(J_o I_1 + J_1 I_o) - I_1 Y_o J_{o\mu}(K_1 - T K_o)] \\
 & + [(Y_{1\mu} - T_{\mu} Y_{o\mu})(\phi_{\mu} I_{1\mu} - \epsilon I_{o\mu}) - (\phi_{\mu} Y_{1\mu} - \alpha Y_{o\mu})(I_{1\mu} + T_{\mu} I_{o\mu})][J_1 I_o J_{o\mu}(K_1 - T K_o) - J_1 K_o J_{o\mu}(I_1 + T I_o) \\
 & - I_1 K_o J_{o\mu}(J_1 - T J_o) - K_1 I_o J_{o\mu}(J_1 - T J_o) - J_o K_1 J_{o\mu}(I_1 + T I_o) + J_o I_1 J_{o\mu}(K_1 - T K_o)] \\
 & + [(\phi_{\mu} K_{1\mu} + \epsilon K_{o\mu})(I_{1\mu} + T_{\mu} I_{o\mu}) - (K_{1\mu} - T_{\mu} K_{o\mu})(\phi_{\mu} I_{1\mu} - \epsilon I_{o\mu})]\{-J_{o\mu} J_1(Y_o I_1 + Y_1 I_o) + J_{o\mu} Y_1(J_o I_1 + J_1 I_o) \\
 & + J_{o\mu} I_1(J_o Y_1 - J_1 Y_o)\} \\
 & + [(Y_{1\mu} - T_{\mu} Y_{o\mu})(\phi_{\mu} J_{1\mu} - \alpha J_{o\mu}) - (\phi_{\mu} Y_{1\mu} - \alpha Y_{o\mu})(J_{1\mu} - T_{\mu} J_{o\mu})][J_1 K_o I_{o\mu}(I_1 + T I_o) - J_1 I_o I_{o\mu}(K_1 - T K_o) \\
 & - K_1 J_o I_{o\mu}(I_1 + T I_o) + I_1 I_{o\mu}(J_o K_1 - J_1 K_o) - K_1 I_o I_{o\mu}(J_1 - T J_o)] \\
 & + [(K_{1\mu} - T_{\mu} K_{o\mu})(\phi_{\mu} J_{1\mu} - \alpha J_{o\mu}) - (\phi_{\mu} K_{1\mu} + \epsilon K_{o\mu})(J_{1\mu} - T_{\mu} J_{o\mu})][J_1 I_{o\mu}(Y_o I_1 + Y_1 I_o) - Y_1 I_{o\mu}(J_o I_1 + J_1 I_o) \\
 & - I_1 I_{o\mu}(J_o Y_1 - J_1 Y_o)]\} (n^* a)
 \end{aligned}
 \tag{21}$$

and

$$\begin{aligned}
 (\text{DEN.}) = \Delta_o^* = & (Y_{1\mu} - T_{\mu} Y_{o\mu})(J_o I_1 + J_1 I_o) \{K_{o\mu}[(J_{1\mu} - T_{\mu} J_{o\mu})(\phi_{\mu} I_{1\mu} - \epsilon I_{o\mu}) - (I_{1\mu} + T_{\mu} I_{o\mu})(\phi_{\mu} J_{1\mu} - J_{o\mu})] \\
 & + J_{o\mu}[(\phi_{\mu} K_{1\mu} + \epsilon K_{o\mu})(I_{1\mu} + T_{\mu} I_{o\mu}) - (K_{1\mu} - T_{\mu} K_{o\mu})(\phi_{\mu} I_{1\mu} - \epsilon I_{o\mu})] \\
 & + I_{o\mu}[(\phi_{\mu} K_{1\mu} + \epsilon K_{o\mu})(J_{1\mu} - T_{\mu} J_{o\mu}) - (K_{1\mu} - T_{\mu} K_{o\mu})(\phi_{\mu} J_{1\mu} - \alpha J_{o\mu})]
 \end{aligned}$$

$$\begin{aligned}
& + (K_{1\mu} - T_{\mu} K_{o\mu})(J_o I_1 + J_1 I_o) \{Y_{o\mu} [(J_{1\mu} - T_{\mu} J_o)(\phi_{\mu} I_{1\mu} - \epsilon I_{o\mu}) - (\phi_{\mu} J_{1\mu} - \alpha J_{o\mu})(I_{1\mu} + T_{\mu} I_{o\mu})] \\
& + J_{o\mu} [(\phi_{\mu} Y_{1\mu} - \alpha Y_{o\mu})(I_{1\mu} + T_{\mu} I_{o\mu}) - (\phi_{\mu} I_{1\mu} - \epsilon I_{o\mu})(Y_{1\mu} - T_{\mu} Y_{o\mu})] \\
& + I_{o\mu} [(\phi_{\mu} Y_{1\mu} - \alpha Y_{o\mu})(J_{1\mu} - T_{\mu} J_{o\mu}) - (\phi_{\mu} J_{1\mu} - \alpha J_{o\mu})(Y_{1\mu} - T_{\mu} Y_{o\mu})]\} (n^* a) \\
& - (J_{1\mu} - T_{\mu} J_{o\mu})(J_o I_1 + J_1 I_o) \{-Y_{o\mu} [(\phi_{\mu} K_{1\mu} + \epsilon K_{o\mu})(I_{1\mu} + T_{\mu} I_{o\mu}) - (K_{1\mu} - T_{\mu} K_{o\mu})(\phi_{\mu} I_{1\mu} - \epsilon I_{o\mu})] \\
& + K_{o\mu} [(\phi_{\mu} Y_{1\mu} - \alpha Y_{o\mu})(I_{1\mu} + T_{\mu} I_{o\mu}) - (Y_{1\mu} - T_{\mu} Y_{o\mu})(\phi_{\mu} I_{1\mu} - \epsilon I_{o\mu})] \\
& + I_{o\mu} [(\phi_{\mu} Y_{1\mu} - \alpha Y_{o\mu})(K_{1\mu} - T_{\mu} K_{o\mu}) - (Y_{1\mu} - T_{\mu} Y_{o\mu})(\phi_{\mu} K_{1\mu} + \epsilon K_{o\mu})]\} (n^* a) \\
& + (I_{1\mu} + T_{\mu} I_{o\mu})(J_o I_1 + J_1 I_o) \{Y_{o\mu} [(K_{1\mu} - T_{\mu} K_{o\mu})(\phi_{\mu} J_{1\mu} - \alpha J_{o\mu}) - (\phi_{\mu} K_{1\mu} + \epsilon K_{o\mu})(J_{1\mu} - T_{\mu} J_{o\mu})] \\
& - K_{o\mu} [(Y_{1\mu} - T_{\mu} Y_{o\mu})(\phi_{\mu} J_{1\mu} - \alpha J_{o\mu}) - (\phi_{\mu} Y_{1\mu} - \alpha Y_{o\mu})(J_{1\mu} - T_{\mu} J_{o\mu})] \\
& - J_{o\mu} [(\phi_{\mu} Y_{1\mu} - \alpha Y_{o\mu})(K_{1\mu} - T_{\mu} K_{o\mu}) - (Y_{1\mu} - T_{\mu} Y_{o\mu})(\phi_{\mu} K_{1\mu} + \epsilon K_{o\mu})]\} (n^* a)
\end{aligned}
\tag{22}$$

In these equations, such terms as  $J_{1\mu}$ ,  $I_{o\mu}$ ,  $K_1$ , and  $Y_o$ , etc., represent the Bessel functions  $J_{(k+1)}(\mu n^* a)$ ,  $I_k(\mu n^* a)$ ,  $K_{(k+1)}(n^* a)$ , and  $Y_k(n^* a)$ , etc.; in addition,

$$T = T^* = k/(n^* a) \quad , \tag{23}$$

$$T_{\mu} = T_{\mu}^* = k/(\mu n^* a) \quad , \tag{24}$$

$$\alpha = \alpha^* \quad , \tag{25}$$

$$\epsilon = \epsilon^* \quad , \tag{26}$$

and

$$\phi_{\mu} = \phi_{\mu}^* = (1 - \nu)/(\mu n^* a) \quad (27)$$

A much more concise expression for transmissibility can be obtained by the principle of reciprocity as the magnitude of the displacement of the plate at the radius  $r = \mu a$  divided by the displacement of the plate boundary ( $r = a$ ) when the boundary is vibrated sinusoidally. The simple expression that can be obtained is as follows:

$$T = \left| \frac{J_1(n^* a) I_0(\mu n^* a) + I_1(n^* a) J_0(\mu n^* a)}{(J_1 I_0 + I_1 J_0)(n^* a)} \right| \quad (28)$$

Representative calculations of transmissibility  $T$  are plotted in Figs. 2-6 for values of  $\mu = 0.2, 0.5, 0.75, 0.2548$  and  $0.379$ ;  $\nu = 1/3$ , and  $\delta_E = \delta_G = 0.01, 0.1$ , and  $1.0$ . In these figures, the horizontal axis is  $(na)$ --a real dimensionless quantity that is proportional to the square root of frequency. Only the symmetrical plate modes ( $k = 0$ ) contribute to transmissibility. Whereas it is true that all other plate modes are excited by the noncentral force, the net upward and downward transmitted forces that they generate at the clamped plate boundary cancel one another exactly.

The transmissibility curves of Figs. 2-4 ( $\mu = 0.2, 0.5, 0.75$ ) exhibit peak values at the symmetrical plate resonances--the extent of the amplification depending on the plate damping, the largest value of which is considered as a hypothetical case since the dynamic Young's and shear moduli associated with such high damping would not be constant, as assumed here, but would increase with frequency.<sup>18</sup> In all cases, transmissibility is equal to unity at low frequencies, as should be expected. Also as expected, the appearance of the transmissibility curves when  $\mu = 0.2$  (Fig. 2) resembles those obtained previously for a centrally driven clamped plate.<sup>20</sup> In Fig. 5, where  $\mu = 0.379$ ,

the second plate resonance is not excited because the impressed force then lies on a nodal circle of the mode; rather, in its place a broad region of attenuation where  $T < 1.0$  is introduced between bounds that differ in frequency by an approximate factor of 4.5. Again, in Fig. 6, when  $\mu = 0.2548$ , the third plate resonance is not excited because the impressed force coincides with a nodal circle of the mode; rather, in its place is a broad region of attenuation that extends between bounds that differ in frequency by an approximate factor of 2.7.

Should the plate be driven by two vibratory forces of like magnitude and phase at two arbitrary points, radii  $\mu_1 a$  and  $\mu_2 a$ , then the resultant force transmissibility is obtained by writing the transmissibility for a single force in the form

$$T = |(a + jb)_\mu| \quad ; \quad (29)$$

so that, for the dual-force excitation, transmissibility is given simply by the equation

$$T_{1,2} = \frac{1}{2} \left| [(a + jb)_{\mu_1} + (a + jb)_{\mu_2}] \right| \quad . \quad (30)$$

Representative calculations of transmissibility  $T_{1,2}$  for dual-force excitation with the point forces applied at the pairs of radii 0.2944a, 0.490a, and 0.2547a, 0.583a, are shown in Figs. 7 and 8, respectively. These locations were chosen judiciously to eliminate evidence of the second and third plate resonances. Rather, in their place, regions of attenuation have been introduced between bounds that differ in frequency by the approximate factors of 5.0 (Fig. 7) and 4.0--or, discounting the single peak where  $na = 6.3$  (Fig. 8) by a factor of 10.5. In these, and in all subsequent calculations, values of  $k$  in the range of at least 1-15 were considered.



### III. DRIVING-POINT IMPEDANCE AT ARBITRARY LOCATION ON PLATE

The driving-point impedance  $Z_\mu$  of the plate at the arbitrary radius  $r = \mu a$ , when normalized by division by the impedance of a lumped mass equal to the plate mass  $M_p$ , can be written as

$$\frac{Z_\mu}{j\omega M_p} = -1/(\text{DEN.}) \quad (31)$$

where

$$(\text{DEN.}) = \left( \frac{n^* a}{2\mu} \right) \left\{ \frac{\Xi_0^*}{\Delta_0} + 2 \sum_{k=1,2,3,\dots}^{\infty} \frac{\Xi_k^*}{\Delta_k} \right\} \quad (32)$$

In Eq. (32),  $\Xi_k^*$  is given by the equation

$$\begin{aligned} \Xi_k^* = & \{ [(Y_{1\mu} - T_{\mu} Y_{\mu}) (\phi_{\mu} J_{1\mu} - \alpha J_{\mu}) - (\phi_{\mu} Y_{1\mu} - \alpha Y_{\mu}) (J_{1\mu} - T_{\mu} J_{\mu})] [I_{\mu} K_{\mu} (J I_1 + I J_1) + I_{\mu}^2 (J K_1 - K J_1) - J_{\mu} I_{\mu} (I K_1 + K I_1)] \\ & + [(\phi_{\mu} K_{1\mu} + \epsilon K_{\mu}) (I_{1\mu} + T_{\mu} I_{\mu}) - (K_{1\mu} - T_{\mu} K_{\mu}) (\phi_{\mu} I_{1\mu} - \epsilon I_{\mu})] [-J_{\mu}^2 (Y I_1 + I Y_1) + J_{\mu} I_{\mu} (J Y_1 - Y J_1) + J_{\mu} Y_{\mu} (I J_1 + J I_1)] \\ & + [(\phi_{\mu} Y_{1\mu} - \alpha Y_{\mu}) (I_{1\mu} + T_{\mu} I_{\mu}) - (Y_{1\mu} - T_{\mu} Y_{\mu}) (\phi_{\mu} I_{1\mu} - \epsilon I_{\mu})] [J_{\mu}^2 (K I_1 + I K_1) - J_{\mu} K_{\mu} (J I_1 + I J_1) - J_{\mu} I_{\mu} (J K_1 - K J_1)] \\ & + [(\phi_{\mu} J_{1\mu} - \alpha J_{\mu}) (I_{1\mu} + T_{\mu} I_{\mu}) - (J_{1\mu} - T_{\mu} J_{\mu}) (\phi_{\mu} I_{1\mu} - \epsilon I_{\mu})] [-J_{\mu} Y_{\mu} (K I_1 + I K_1) + J_{\mu} K_{\mu} (Y I_1 + I Y_1) - K_{\mu} I_{\mu} (J Y_1 - Y J_1) \\ & \quad + Y_{\mu} I_{\mu} (J K_1 - K J_1)] \\ & + [(\phi_{\mu} J_{1\mu} - \alpha J_{\mu}) (K_{1\mu} - T_{\mu} K_{\mu}) - (J_{1\mu} - T_{\mu} J_{\mu}) (\phi_{\mu} K_{1\mu} + \epsilon K_{\mu})] [J_{\mu} I_{\mu} (Y I_1 + I Y_1) - Y_{\mu} I_{\mu} (J I_1 + I J_1) \\ & \quad - I_{\mu}^2 (J Y_1 - Y J_1)] \} (n^* a) \cos k\theta \quad (33) \end{aligned}$$

The parameter  $\Delta_o^*$  is given by Eq. (22),  $\Xi_o^*$  is given by Eq. (33) in which such terms as  $Y_{1\mu}$  and  $Y_\mu$  representing  $Y_{(k+1)}(\mu^*a)$  and  $Y_k(\mu^*a)$  are replaced by  $Y_1(\mu^*a)$  and  $Y_o(\mu^*a)$ , and such terms as  $J, I_1$  representing  $J_k(n^*a)$ ,  $I_{(k+1)}(n^*a)$  are replaced by  $J_o(n^*a)$ ,  $I_1(n^*a)$ . Again,  $\Delta_k^*$  is given by Eq. (22) in which such terms as  $Y_{1\mu}$  and  $Y_{o\mu}$  now become  $Y_{(k+1)}(\mu^*a)$  and  $Y_k(\mu^*a)$  so that, for example, the first term of Eq. (22) should read as follows:

$$\begin{aligned}
 & (Y_{(k+1)\mu} - T_\mu Y_{k\mu})(n^*a) (J_k I_{(k+1)} + I_k J_{(k+1)})(n^*a) \times \\
 & \{K_{k\mu} [(J_{(k+1)\mu} - T_\mu J_{k\mu})(\phi_\mu I_{(k+1)\mu} - \epsilon I_{k\mu}) - (I_{(k+1)\mu} + T_\mu I_{k\mu})(\phi_\mu J_{(k+1)\mu} - \alpha J_{k\mu})] \\
 & + J_{k\mu} [(\phi_\mu K_{(k+1)\mu} + \epsilon K_{k\mu})(I_{(k+1)\mu} + T_\mu I_{k\mu}) - (K_{(k+1)\mu} - T_\mu K_{k\mu})(\phi_\mu I_{(k+1)\mu} - \epsilon I_{k\mu})] \\
 & + I_{k\mu} [(\phi_\mu K_{(k+1)\mu} + \epsilon K_{k\mu})(J_{(k+1)\mu} - T_\mu J_{k\mu}) - (K_{(k+1)\mu} - T_\mu K_{k\mu})(\phi_\mu J_{(k+1)\mu} - \alpha J_{k\mu})]\} (n^*a) \quad (34)
 \end{aligned}$$

Here, as before, the terms  $T_\mu$ ,  $\phi_\mu$ ,  $\alpha$ , and  $\epsilon$  are given by Eqs. (24)-(27).

Representative calculations of  $|Z_\mu/j\omega M_p|$  are plotted in Figs. 9-11 for values of  $\mu = 0.2, 0.5$ , and  $0.75$ ,  $\nu = 1/3$ , and  $\delta_E = \delta_G = 0.01, 0.1$ , and  $1.0$ . Evidence is now seen of every mode of plate vibration--both symmetrical and nonsymmetrical. At low frequencies, the plate impedance is very large and springlike--so that the normalized impedance diminishes inversely in proportion to  $\omega^2$ . The impedance alternately exhibits minima (plate resonances) and maxima (plate antiresonances) that lie almost symmetrically about the heavily damped impedance curve for which  $\delta_E = \delta_G = 1.0$ .

## IV. VIBRATION OF THE MASS-LOADED PLATE

The driving-point impedance  $Z_{\mu m}$  and the force transmissibility  $T_{\mu m}$  of the plate of Fig. 1 when it is loaded by a mass  $M$  at the point of application of the noncentral force follow directly from the foregoing results. Thus, since there must be continuity of motion between  $M$  and the plate, it follows that, if the loading mass is  $\gamma$  times greater than the plate mass  $M_p$ ,

$$Z_{\mu m} = j\omega M + Z_{\mu} \quad (35)$$

or

$$\frac{Z_{\mu m}}{j\omega M_p} = \gamma + \frac{Z_{\mu}}{j\omega M_p} \quad (36)$$

and

$$T_{\mu m} = T_{\mu} \left| \frac{(Z_{\mu}/j\omega M_p)}{\gamma + (Z_{\mu}/j\omega M_p)} \right| \quad (37)$$

Calculations of  $T_{\mu m}$  for a value of  $\gamma = 1.0$ ,  $\nu = 1/3$ , and  $\mu = 0.2, 0.5$  and  $0.75$ , are plotted in Figs. 12-14 for values of  $\delta_E = \delta_G = 0.01, 0.1$ , and  $1.0$ . Now, because the nonsymmetric plate modes are excited due to the presence of the noncentral mass loading, essentially twice the number of resonances are excited than before (Figs. 2-4).

Companion plots of the normalized driving-point impedance  $|Z_{\mu m}/j\omega M_p|$  are presented in Figs. 15-17. Again, essentially twice the number of resonances (minima of impedance, maxima of transmissibility) are observed. Notice how, in all these figures (Figs. 12-17), the plate resonances are shifted to lower frequencies by the mass loading (such a shift is always observed when a structure is mass loaded<sup>18,20</sup>); and how, at low frequencies, the plate impedance

remains springlike in character. Also notice that the normalized impedances of the plate at higher frequencies exhibit only limited fluctuations about the value unity; this is to say, the impressed force is primarily presented with the impedance of the loading mass--the impedance of the plate being negligible by comparison.

#### V. VIBRATION OF A PLATE DRIVEN OFF CENTER AT A POINT TO WHICH A DYNAMIC VIBRATION ABSORBER IS ATTACHED

In this situation, the force transmissibility  $T_a$  to the plate boundary can be written as

$$T_a = T_\mu \left| \frac{(Z_\mu / j\omega M_P)}{[\Psi^* + (Z_\mu / j\omega M_P)]} \right|, \quad (38)$$

where  $T_\mu$  and  $(Z_\mu / j\omega M_P)$  are the force transmissibility and the normalized driving-point impedance of the plate at the driving point located at the arbitrary distance  $\mu a$  from the plate center. The complex parameter  $\Psi^*$  is given by the relatively simple equation

$$\Psi^* = \frac{\gamma_a [1 + 2j(\omega_m / \omega_a) \Omega_m \delta_R]}{[1 - (\omega_m / \omega_a)^2 \Omega_m^2 + 2j(\omega_m / \omega_a) \Omega_m \delta_R]}, \quad (39)$$

where

$$\gamma_a = M_a / M_P \quad (40)$$

and

$$\Omega_m = \frac{\omega}{\omega_{11}} = \frac{\omega}{\omega_m} = \frac{(na)^2}{(3.1962)^2} \quad (41)$$

Here,  $M_a$  is the absorber mass and  $\omega_{11}$  is the fundamental plate frequency to which, in this instance, but not necessarily, the absorber is tuned. [For example, if the absorber is tuned to the second or third plate resonance, Eq. (41) would remain relevant but the number (3.1962) would be replaced by the numbers (6.3064) or (9.4395).] The quantities  $(\omega_m/\omega_a)^{-1}$  and  $\delta_R$  are design parameters of the dynamic absorber and they must be chosen carefully if the full potential of the absorber is to be realized. For example, if  $\mu$  is small and if the mass ratio  $\gamma_a = 0.1$  or  $0.25$ , then  $(\omega_a/\omega_m) = 0.698$ ,  $\delta_R = 0.408$ , or  $(\omega_a/\omega_m) = 0.465$ ,  $\delta_R = 0.549$ , respectively.<sup>21</sup> These values yield near-optimum conditions for which the two maxima in the transmissibility curve take essentially equal values a little to each side of the fundamental plate resonance. They assume that the plate damping factors  $\delta_E = \delta_G = 0.01$ , a value that is adopted for the remainder of this section.

Representative calculations of the transmissibility  $T_a$  are plotted in Figs. 18 and 19 for a value of  $\mu = 0.2$  and for pairs of values of  $(\omega_a/\omega_m)$  and  $\delta_R$  that differ slightly from those previously specified; namely,  $(\omega_a/\omega_m) = 0.698$ ,  $\delta_R = 0.462$ , and  $(\omega_a/\omega_m) = 0.493$ ,  $\delta_R = 0.546$ , respectively. The absorbers of Figs. 18 and 19 are seen to be most effective in suppressing the plate resonance to which they are tuned; they also suppress, to some extent, the higher plate resonances--particularly the heavier absorber, which has the larger damping ratio. Thus, at frequencies above the absorber resonance, the absorber mass becomes an almost stationary point from which the absorber dashpot is able to restrain the resonant plate motion, and the force transmissibility across the plate, at higher frequencies. Companion curves for the dynamic absorbers (mass ratios  $\gamma_a = 0.1$  and  $0.25$ ) located at



the radial distance  $0.75a$  from the plate center, for which the plate impedance is approximately 30 times greater than at the radial distance  $0.2a$ , are plotted in Figs. 20 and 21, respectively. Because of the larger value of the plate impedance, to attain equal peak heights near the fundamental plate resonance proved more difficult than usual. Other values of the optimum tuning and damping ratios and the companion values of maximum transmissibility at the fundamental plate resonance are plotted in Fig. 22 as a function of the parameter  $\mu$ .

Should the plate be mass loaded at the point of attachment of the dynamic absorber, then the force transmissibility  $T_{ma}$  to the plate boundary can readily be stated from inspection of Eq. (38) as

$$T_{ma} = T_{\mu m} \left| \frac{(Z_{\mu m}/j\omega M_p)}{[\Psi^* + (Z_{\mu m}/j\omega M_p)]} \right|, \quad (42)$$

where  $(Z_{\mu m}/j\omega M_p)$  and  $T_{\mu m}$  are the normalized driving-point impedance and force transmissibility of the mass-loaded plate [Eqs. (36) and (37)] at the arbitrary driving point distance  $\mu a$  from the plate center. In this situation, the parameter  $\gamma$  (factor by which the loading mass exceeds the plate mass) is equated to 1.0; the same values of  $(\omega_a/\omega_m)$  and  $\delta_R$  (parameters that appear in  $\Psi^*$ ) as before are initially chosen, and then changes are made in their values to equalize the two transmissibility maxima because, to begin with, these maxima will only be approximately equal.

Representative calculations of  $T_{ma}$  are plotted in Figs. 23 and 24 for values of  $\gamma = 1.0$ ,  $\gamma_a = 0.1$ ; and, again, values of  $\mu = 0.2$  and  $0.75$ . Optimum values of  $(\omega_a/\omega_m) = 0.356$ ,  $\delta_R = 0.119$ , and of  $(\omega_a/\omega_m) = 0.761$ ,  $\delta_R = 0.139$ , respectively, are seen to provide equal suppression of the transmissibility peaks at the fundamental plate resonance; now, however, the loading mass

causes the force transmissibility to fall off quite rapidly at all higher frequencies. Again, other values of the optimum tuning and damping ratios, and the companion values of maximum transmissibility are plotted in Fig. 25.

#### ACKNOWLEDGMENTS

Especial thanks are due to Adah A. Wolfe for her help in obtaining the results presented graphically in this report. The investigation was sponsored by the U. S. Naval Sea Systems Command, and this support is acknowledged with gratitude.

## REFERENCES

1. J. H. Michelle, "The Flexure of a Circular Plate," Proc. London Math. Soc. 34, 223-228 (1902).
2. R. J. Roark, "Stresses Produced in a Circular Plate by Eccentric Loading and by a Transverse Couple," The University of Wisconsin Bulletin No. 74, 1-41 (1932).
3. A. M. Sen Gupta, "Bending of a Cylindrically Anisotropic Circular Plate with Eccentric Load," J. Appl. Mech., Trans. Am. Soc. Mech. Engrs., Series E, 19, 9-12 (1952).
4. M. A. Goldberg, T. L. Hoffa, and J. Gorga, Analysis of an Annular Plate Subjected to a Concentrated Load, Polytechnic Institute of Brooklyn, Department of Aerospace Engineering and Applied Mechanics, PIBAL Rept. No. 68-2 (February, 1962).
5. J. Dundurs and T.-M. Lee, "Flexure by a Concentrated Force of the Infinite Plate on a Circular Support," J. Appl. Mech., Trans. Am. Soc. Mech. Engrs., Series E, 30, 225-231 (1963).
6. R. Amon and J. Dundurs, "Supported Plate with Supported Edge Beam," J. Eng. Mech. Divn., Proc. Am. Soc. Civ. Engrs. 94, 731-742 (1968).
7. S. G. Lekhnitskii, Anisotropic Plates, Translated from the Russian by S. W. Tsai and T. Cheron, (Gordon and Breach, 1968), p. 376.
8. R. Amon, O. E. Widera, and R. G. Ahrens, "Problem of the Annular Plate, Simply Supported and Loaded with an Eccentric Concentrated Force," AIAA J. 8, 961-963 (1970).
9. Y. Takeuti and N. Noda, "On a Measurement of Various Shaped Plates by Optical Interference Method," J. Appl. Mech., Trans. Am. Soc. Mech. Engrs., Series E, 37, 1182-1186 (1970).

## REFERENCES -- CONTINUED

10. B. Moustakakis and J. F. Carney, III, "Annular Plate with Supporting Edge Beams," AIAA J. 10, 529-531 (1972).
11. R. Szilard, Theory and Analysis of Plates: Classical and Numerical Methods, (Prentice-Hall, Inc., 1974).
12. R. Ramakrishnan and V. X. Kunukkasseril, "Asymmetric Response of Circular Plates," J. Sound Vib. 34, 489-504 (1974).
13. H. Reissman, "Forced Vibrations of a Circular Plate," J. Appl. Mech., Trans. Am. Soc. Mech. Engrs., Series E, 26, 526-527 (1959).
14. A. J. McLeod and R. E. D. Bishop, The Forced Vibration of Circular Flat Plates, Mech. Engr. Sci, Monograph No. 1, Inst. Mech. Engrs. (London), (1965).
15. A. Kalnins, "On Fundamental Solutions and Green's Functions in the Theory of Elastic Plates," J. Appl. Mech., Trans, Am. Soc. Mech. Engrs., Series E, 33, 31-38 (1966).
16. G. Anderson, "On the Determination of Finite Integral Transforms for Forced Vibrations of Circular Plates," J. Sound Vib. 9, 126-144 (1969).
17. D. S. Potter and C. D. Leedham, "Antisymmetric Vibrations of a Circular Plate," J. Acoust. Soc. Am. 49, 1521-1526 (1971).
18. J. C. Snowdon, Vibration and Shock in Damped Mechanical Systems (John Wiley and Sons, Inc., New York, 1968).
19. R. L. Kerlin and J. C. Snowdon, "Driving-Point Impedances of Cantilever Beams -- Comparison of Measurement and Theory," J. Acoust. Soc. Am. 47, 220-228 (1970).

## REFERENCES -- CONTINUED

20. J. C. Snowdon, "Forced Vibration of Internally Damped Circular and Annular Plates with Clamped Boundaries," J. Acoust. Soc. Am. 50, 846-858 (1971).
21. J. C. Snowdon, "Mechanical Four-Pole Parameters and their Application," J. Sound Vib. 15, 307-323 (1971).



## FIGURE LEGENDS

- Fig. 1 An internally damped circular plate of radius  $a$  that is clamped around its boundary and driven by a vibratory force at an arbitrary distance  $\mu a$  from the plate center.
- Fig. 2 Force transmissibility to the boundary of the plate of Fig. 1; plate damping factors  $\delta_E = \delta_G = 0.01, 0.1, \text{ and } 1.0$ ; the parameter  $\mu = 0.2$ .
- Fig. 3 Force transmissibility to the boundary of the plate of Fig. 1; plate damping factors  $\delta_E = \delta_G = 0.01, 0.1, \text{ and } 1.0$ ; the parameter  $\mu = 0.5$ .
- Fig. 4 Force transmissibility to the boundary of the plate of Fig. 1; plate damping factors  $\delta_E = \delta_G = 0.01, 0.1, \text{ and } 1.0$ ; the parameter  $\mu = 0.75$ .
- Fig. 5 Force transmissibility to the boundary of the plate of Fig. 1; plate damping factors  $\delta_E = \delta_G = 0.01, 0.1, \text{ and } 1.0$ ; the parameter  $\mu = 0.379$ .
- Fig. 6 Force transmissibility to the boundary of the plate of Fig. 1; plate damping factors  $\delta_E = \delta_G = 0.01, 0.1, \text{ and } 1.0$ ; the parameter  $\mu = 0.2548$ .
- Fig. 7 Force transmissibility to the boundary of the plate of Fig. 1 when the plate is driven simultaneously by dual vibratory forces of equal phase and magnitude; plate damping factors  $\delta_E = \delta_G = 0.01, 0.1, \text{ and } 1.0$ ; the parameters  $\mu_1 = 0.2944a$  and  $\mu_2 = 0.490a$ .
- Fig. 8 Force transmissibility to the boundary of the plate of Fig. 1 when the plate is driven simultaneously by dual vibratory forces of

## FIGURE LEGENDS -- CONTINUED

equal phase and magnitude; plate damping factors  $\delta_E = \delta_G = 0.01$ , 0.1, and 1.0; the parameters  $\mu_1 = 0.2547a$  and  $\mu_2 = 0.583a$ .

- Fig. 9 Normalized driving-point impedance of the plate of Fig. 1; plate damping factors  $\delta_E = \delta_G = 0.01$ , 0.1, and 1.0; the parameter  $\mu = 0.2$ .
- Fig. 10 Normalized driving-point impedance of the plate of Fig. 1; plate damping factors  $\delta_E = \delta_G = 0.01$ , 0.1, and 1.0; the parameter  $\mu = 0.5$ .
- Fig. 11 Normalized driving-point impedance of the plate of Fig. 1; plate damping factors  $\delta_E = \delta_G = 0.01$ , 0.1, and 1.0; the parameter  $\mu = 0.75$ .
- Fig. 12 Force transmissibility to the boundary of the plate of Fig. 1 when the plate is loaded at the driving point by a lumped mass equal to the plate mass ( $\gamma = 1.0$ ); plate damping factors  $\delta_E = \delta_G = 0.01$ , 0.1, and 1.0; the parameter  $\mu = 0.2$ .
- Fig. 13 Force transmissibility to the boundary of the plate of Fig. 1 when the plate is loaded at the driving point by a lumped mass equal to the plate mass ( $\gamma = 1.0$ ); plate damping factors  $\delta_E = \delta_G = 0.01$ , 0.1, and 1.0; the parameter  $\mu = 0.5$ .
- Fig. 14 Force transmissibility to the boundary of the plate of Fig. 1 when the plate is loaded at the driving point by a lumped mass equal to the plate mass ( $\gamma = 1.0$ ); plate damping factors  $\delta_E = \delta_G = 0.01$ , 0.1, and 1.0; the parameter  $\mu = 0.75$ .
- Fig. 15 Normalized driving-point impedance of the plate of Fig. 1 when the plate is loaded at the driving point by a lumped mass equal to the plate mass ( $\gamma = 1.0$ ); plate damping factors  $\delta_E = \delta_G = 0.01$ , 0.1, and 1.0; the parameter  $\mu = 0.2$ .

## FIGURE LEGENDS -- CONTINUED

Fig. 16 Normalized driving-point impedance of the plate of Fig. 1 when the plate is loaded at the driving point by a lumped mass equal to the plate mass ( $\gamma = 1.0$ ); plate damping factors  $\delta_E = \delta_G = 0.01, 0.1$ , and  $1.0$ ; the parameter  $\mu = 0.5$ .

Fig. 17 Normalized driving-point impedance of the plate of Fig. 1 when the plate is loaded at the driving point by a lumped mass equal to the plate mass ( $\gamma = 1.0$ ); plate damping factors  $\delta_E = \delta_G = 0.01, 0.1$ , and  $1.0$ ; the parameter  $\mu = 0.75$ .

Fig. 18 Force transmissibility to the boundary of the plate of Fig. 1 when a dynamic vibration absorber is attached to the plate at the arbitrary driving point. Mass ratio  $\gamma_a = 0.1$ ; optimum tuning and damping ratios  $(\omega_a/\omega_m) = 0.698$ ,  $\delta_R = 0.462$ ; the parameter  $\mu = 0.2$ ; the plate damping factors  $\delta_E = \delta_G = 0.01$ .

Fig. 19 Force transmissibility to the boundary of the plate of Fig. 1 when a dynamic vibration absorber is attached to the plate at the arbitrary driving point. Mass ratio  $\gamma_a = 0.25$ ; optimum tuning and damping ratios  $(\omega_a/\omega_m) = 0.493$ ,  $\delta_R = 0.546$ . The parameter  $\mu = 0.2$ ; the plate damping factors  $\delta_E = \delta_G = 0.01$ .

Fig. 20 Force transmissibility to the boundary of the plate of Fig. 1 when a dynamic vibration absorber is attached to the plate at the arbitrary driving point. Mass ratio  $\gamma_a = 0.1$ ; optimum tuning and damping ratios  $(\omega_a/\omega_m) = 0.980$ ,  $\delta_R = 0.089$ . The parameter  $\mu = 0.75$ ; the plate damping factors  $\delta_E = \delta_G = 0.01$ .

Fig. 21 Force transmissibility to the boundary of the plate of Fig. 1 when a dynamic vibration absorber is attached to the plate at the

## FIGURE LEGENDS -- CONTINUED

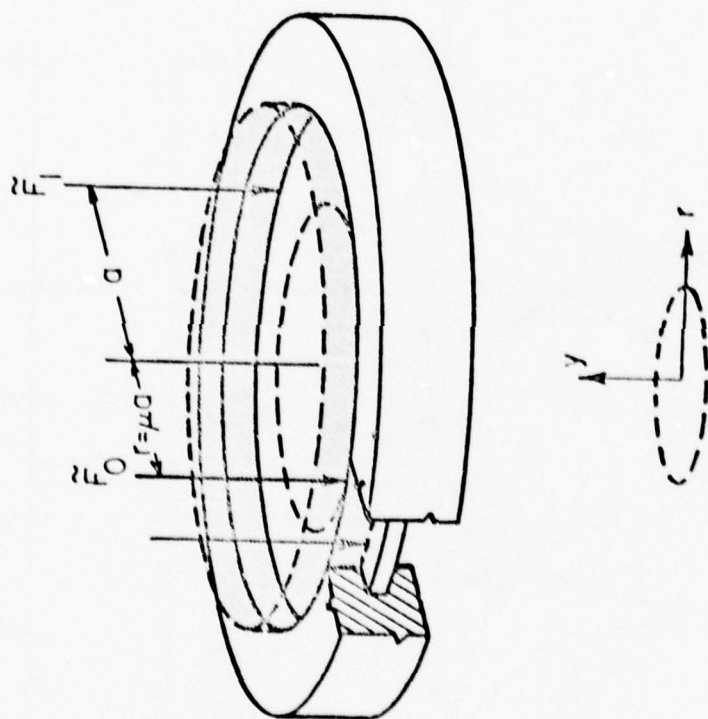
arbitrary driving point. Mass ratio  $\gamma_a = 0.25$ ; optimum tuning and damping ratios  $(\omega_a/\omega_m) = 0.950$ ,  $\delta_R = 0.182$ . The parameter  $\mu = 0.75$ ; the plate damping factors  $\delta_E = \delta_G = 0.01$ .

Fig. 22 Optimum values of the tuning and damping ratios  $(\omega_a/\omega_m)$  and  $\delta_R$ , and the companion values of the maximum transmissibility  $T_{\max}$  at the fundamental plate resonance plotted as a function of the parameter  $\mu$ ; the plate damping factors  $\delta_E = \delta_G = 0.01$ . For the dashed- and solid-line curves, the mass ratio  $\gamma_a = 0.1$  and  $0.25$ , respectively.

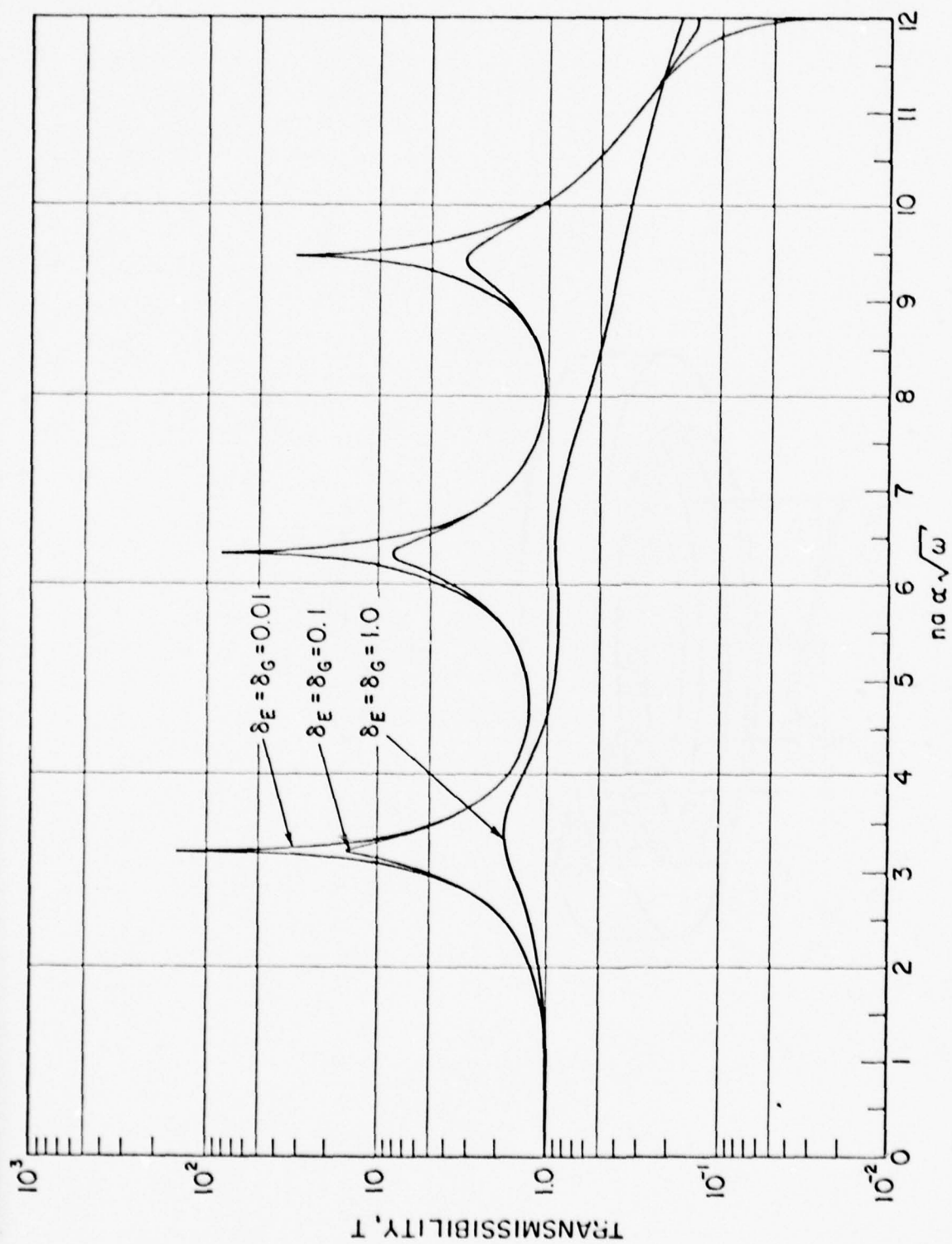
Fig. 23 Force transmissibility to the boundary of the plate of Fig. 1 when both a lumped mass and a dynamic vibration absorber are attached to the plate at the arbitrary driving point. Mass ratios  $\gamma = 1.0$ ,  $\gamma_a = 0.1$ ; optimum tuning and damping ratios  $(\omega_a/\omega_m) = 0.356$ ,  $\delta_R = 0.119$ . The parameter  $\mu = 0.2$ ; the plate damping factors  $\delta_E = \delta_G = 0.01$ .

Fig. 24 Force transmissibility to the boundary of the plate of Fig. 1 when both a lumped mass and a dynamic vibration absorber are attached to the plate at the arbitrary driving point. Mass ratios  $\gamma = 1.0$ ,  $\gamma_a = 0.1$ ; optimum tuning and damping ratios  $(\omega_a/\omega_m) = 0.761$ ,  $\delta_R = 0.139$ . The parameter  $\mu = 0.75$ ; the plate damping factors  $\delta_E = \delta_G = 0.01$ .

Fig. 25 Optimum values of the tuning and damping ratios  $(\omega_a/\omega_m)$  and  $\delta_R$ , and the companion values of the maximum transmissibility  $T_{\max}$  at the fundamental plate resonance plotted as a function of the parameter  $\mu$ ; the plate damping factors  $\delta_E = \delta_G = 0.01$ . For the dashed- and solid-line curves, the mass ratio  $\gamma_a = 0.1$  and  $0.25$ , respectively. For both curves, the mass ratio  $\gamma = 1.0$ .







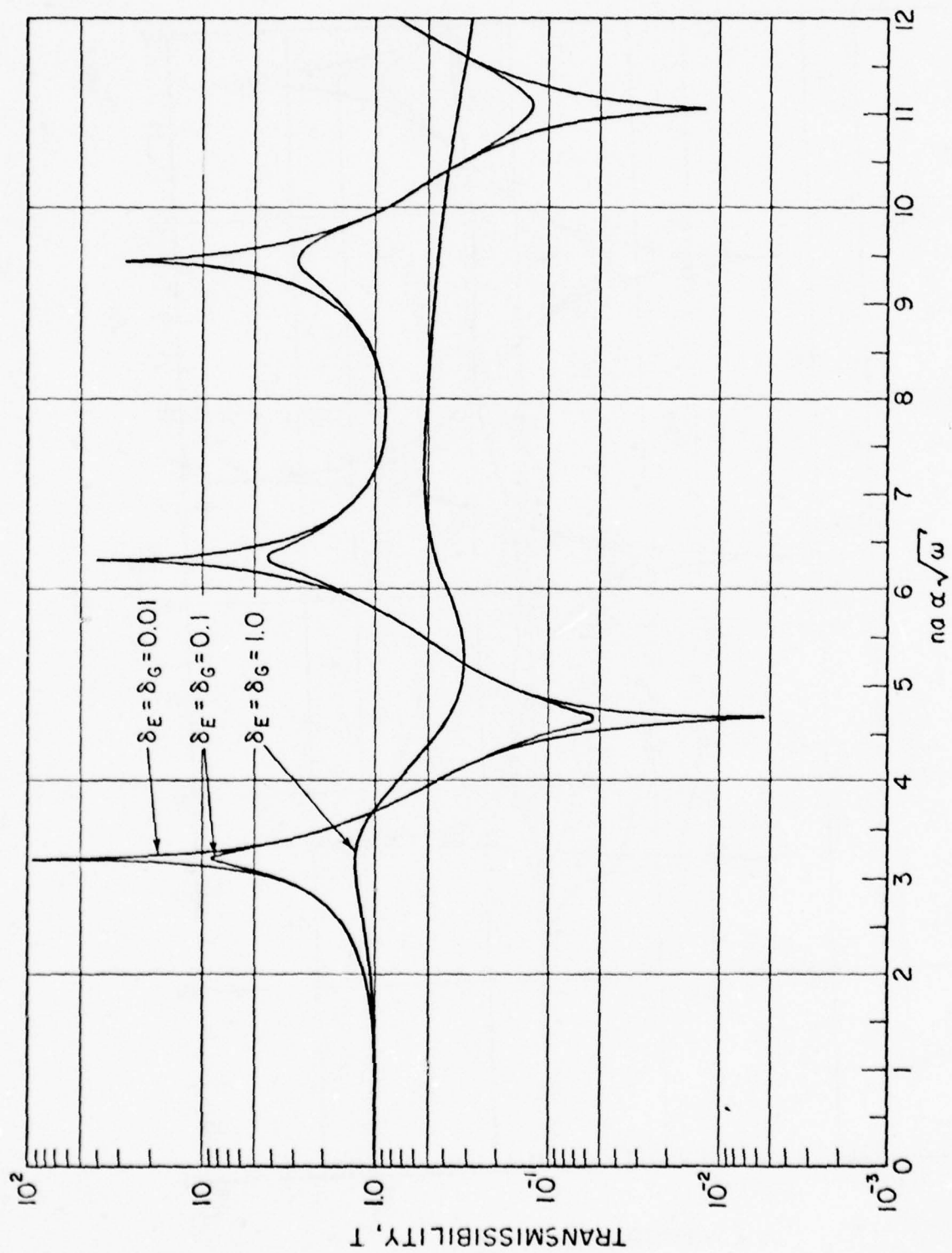


FIG. 3

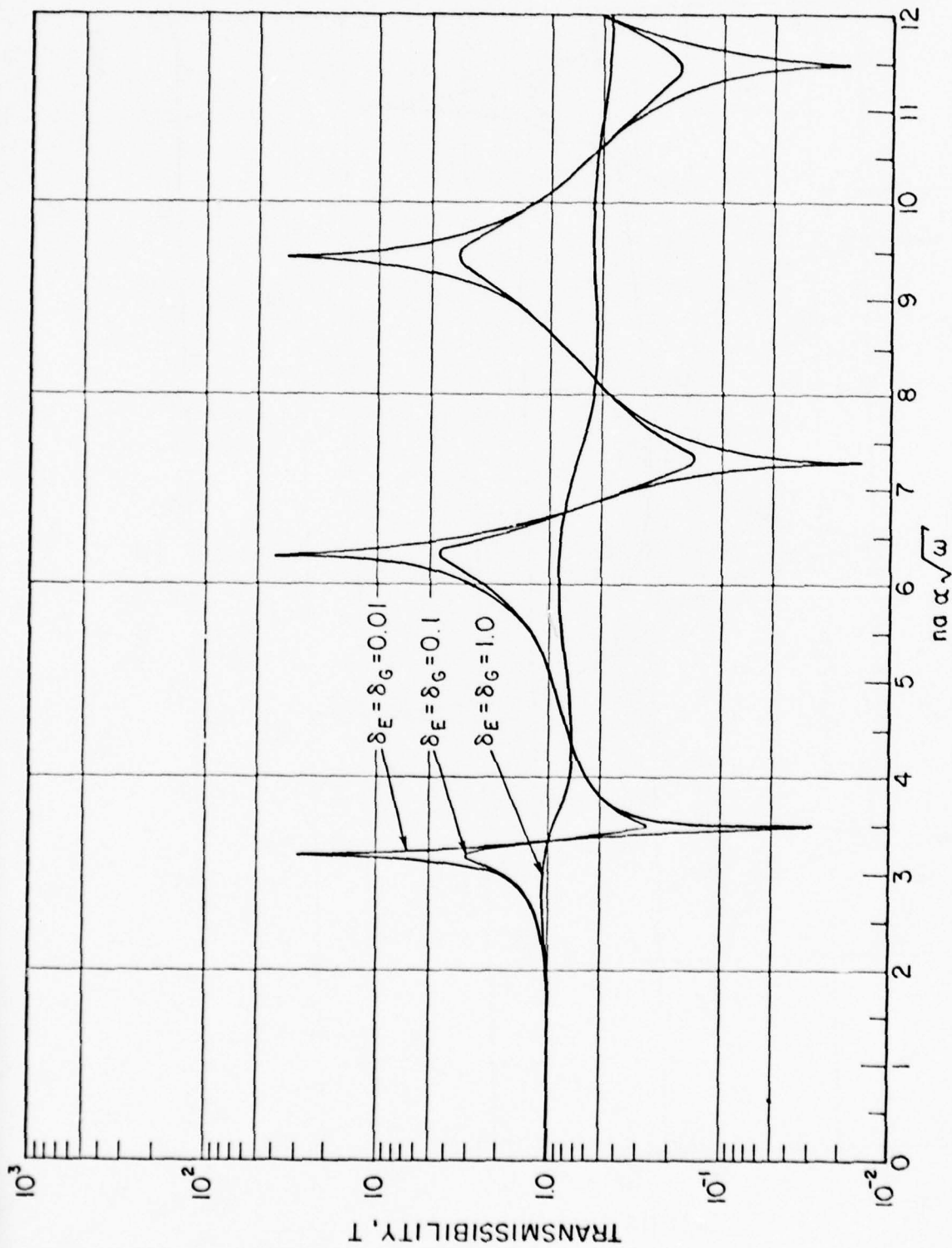
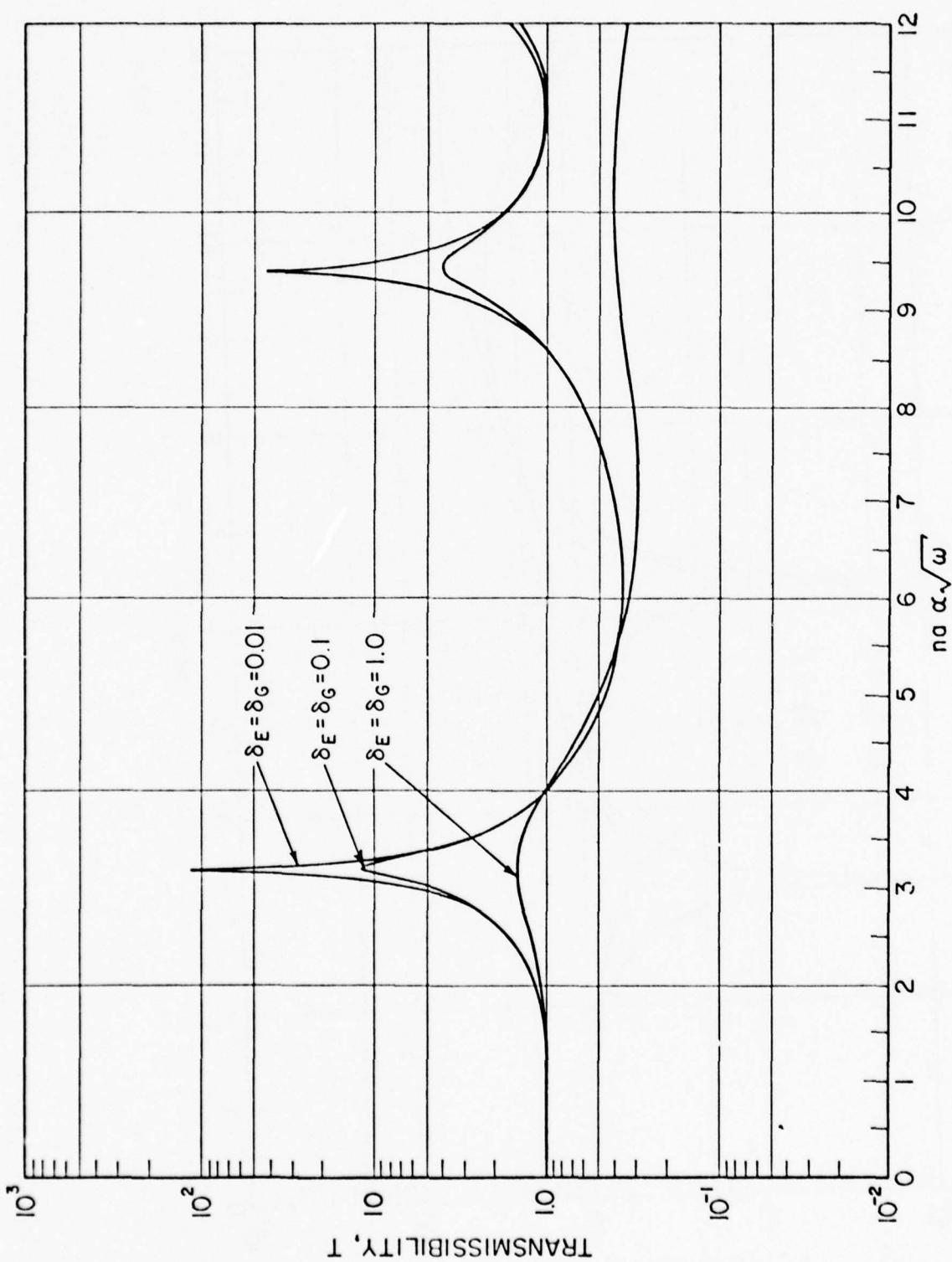
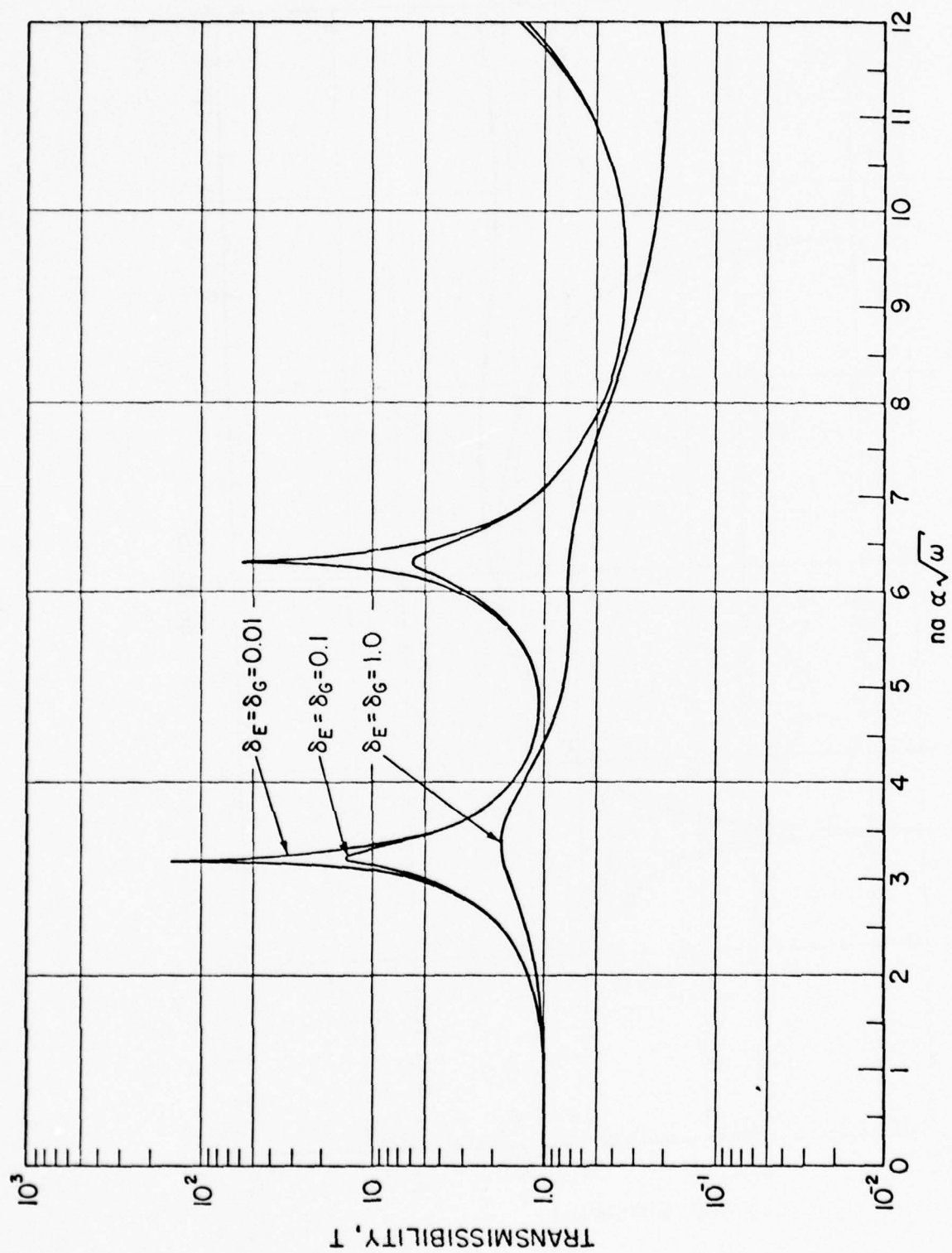


FIG. 4







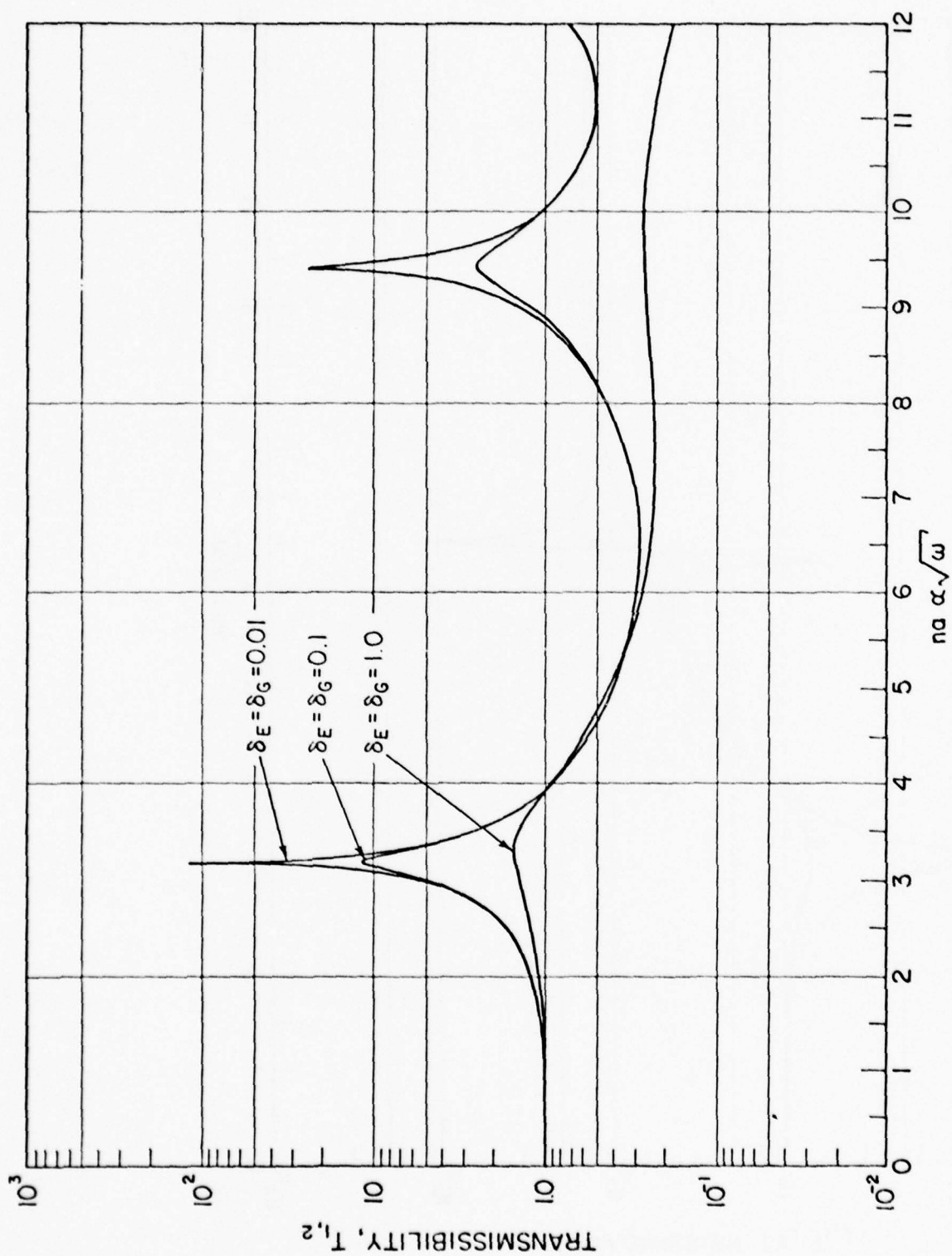


FIG. 7

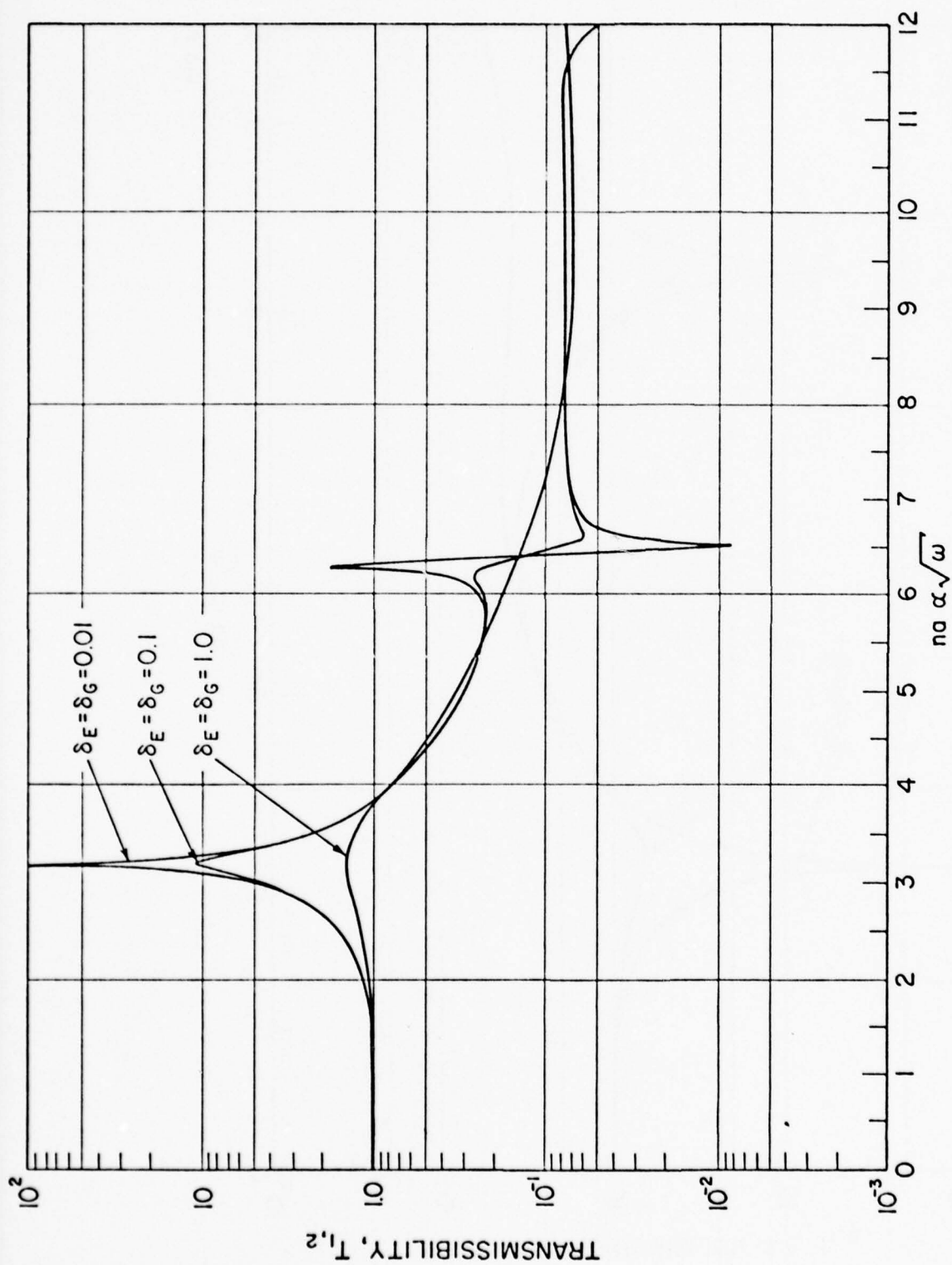
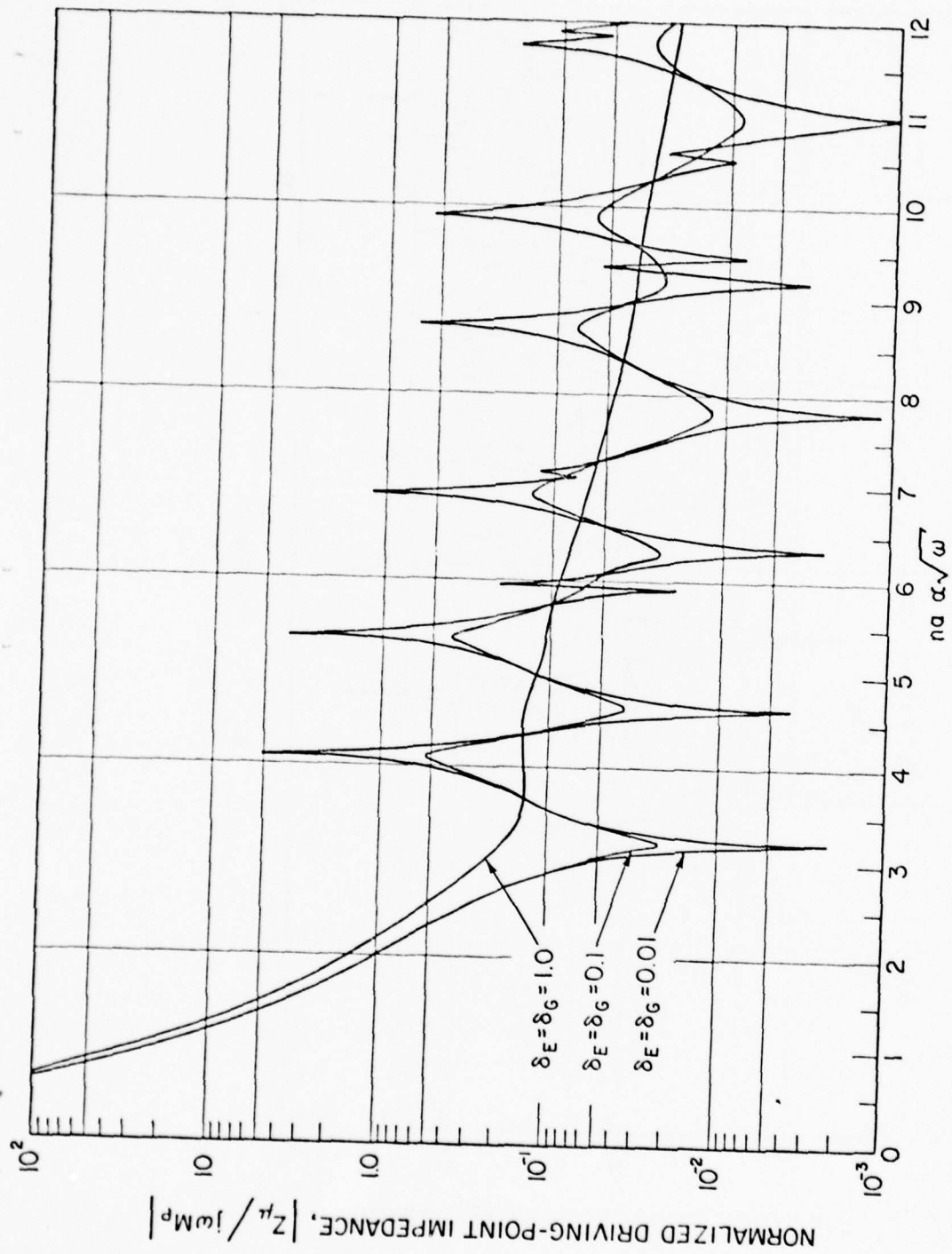


FIG. 8



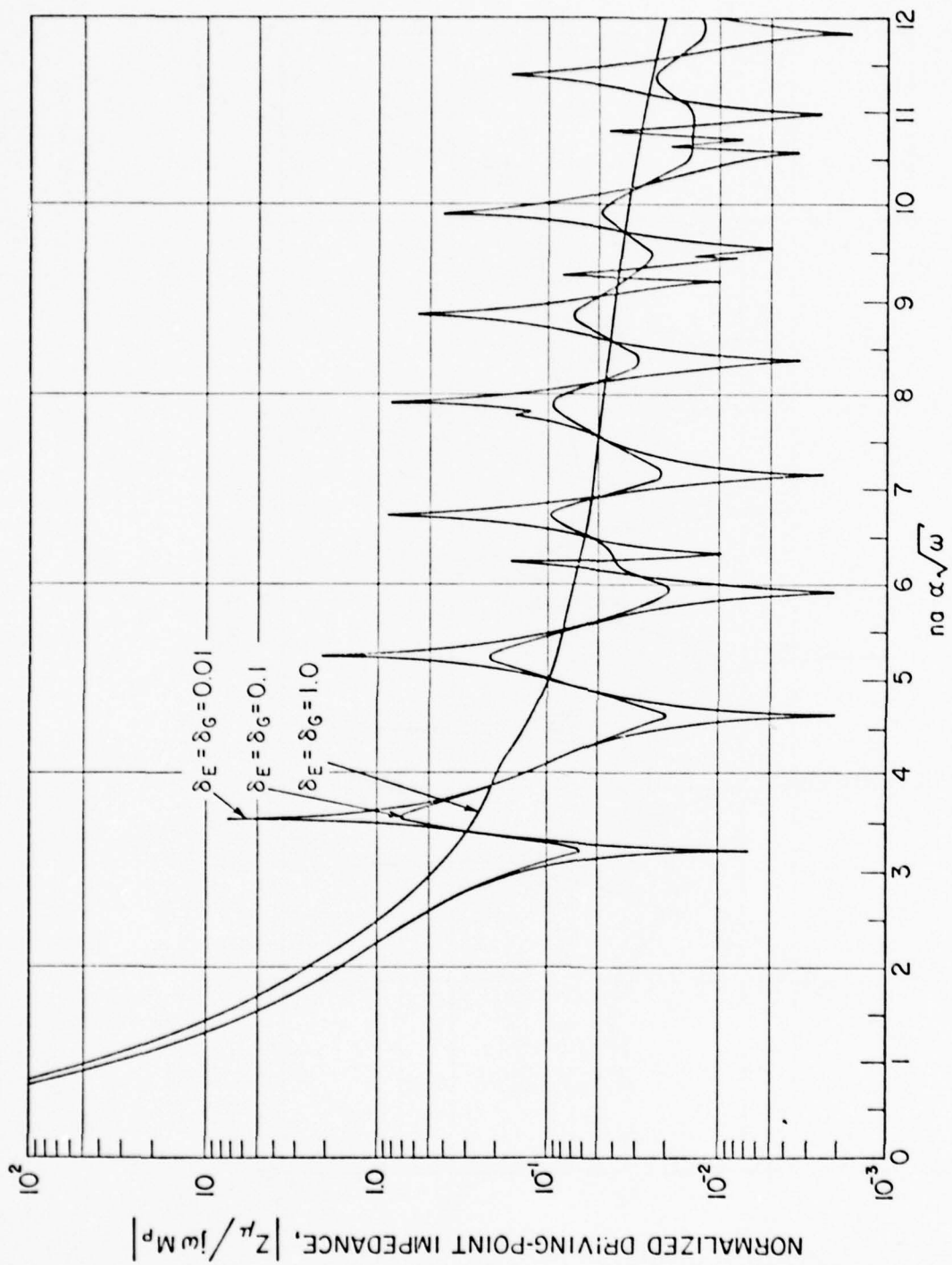
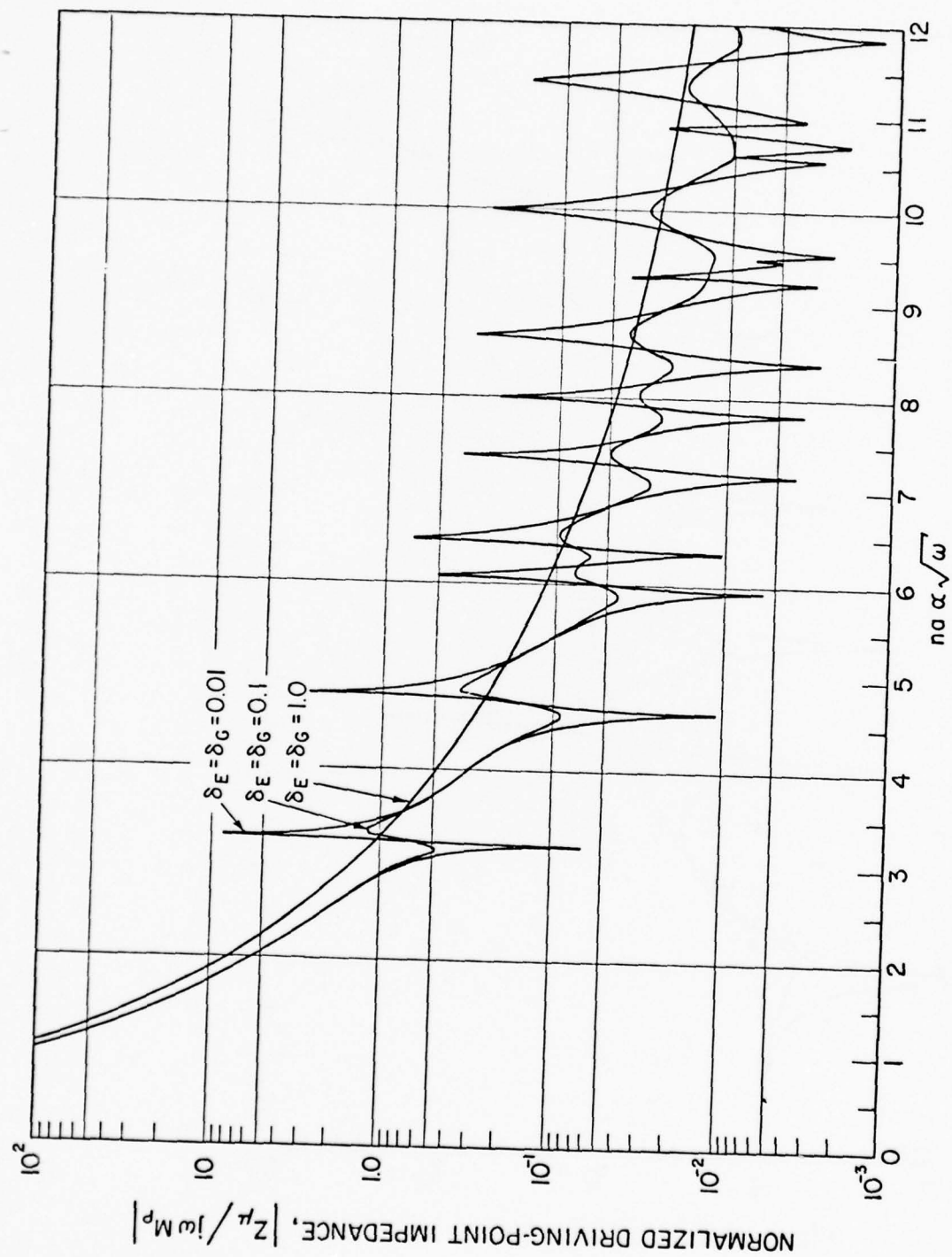


FIG. 10





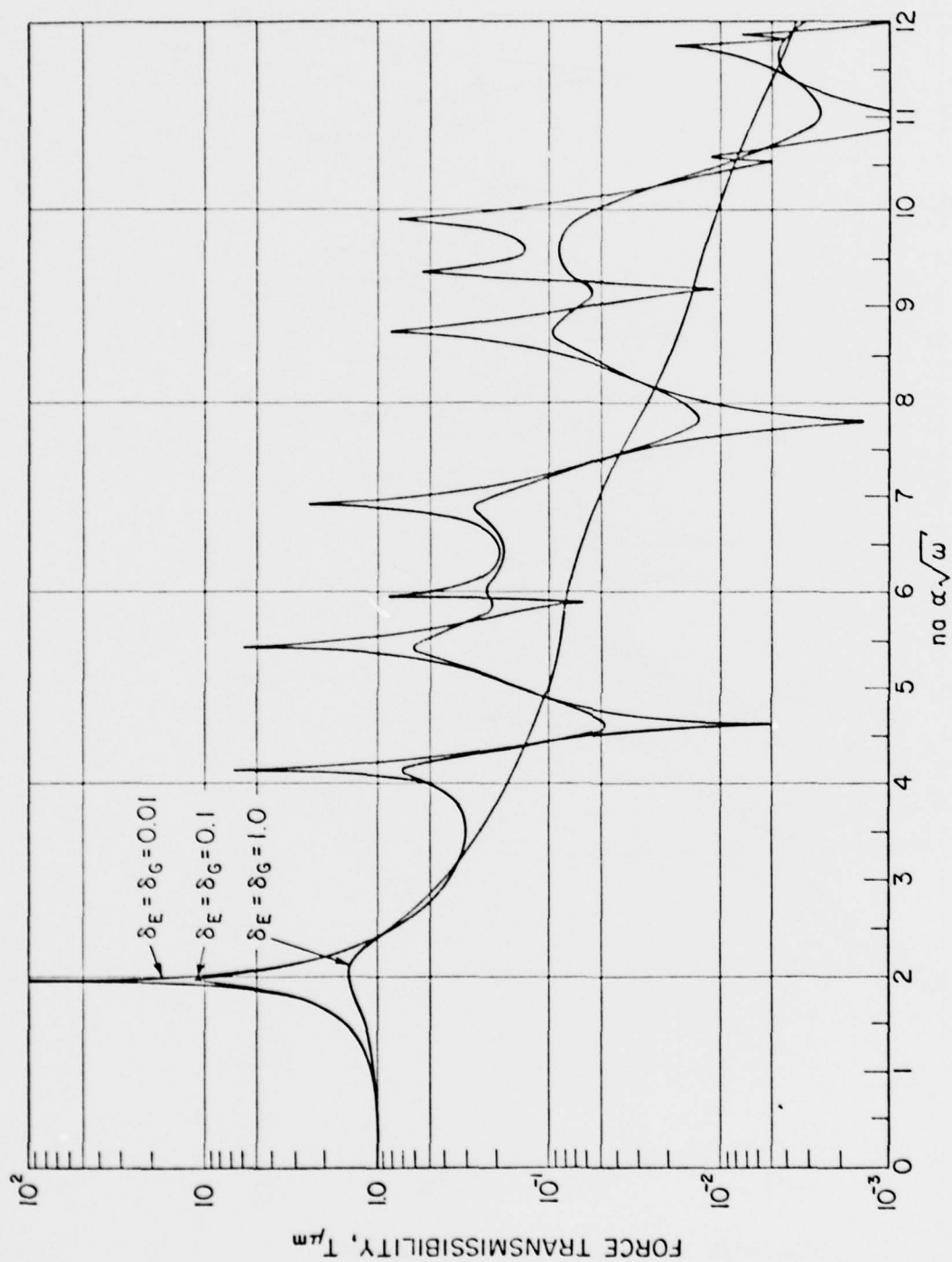


FIG. 12

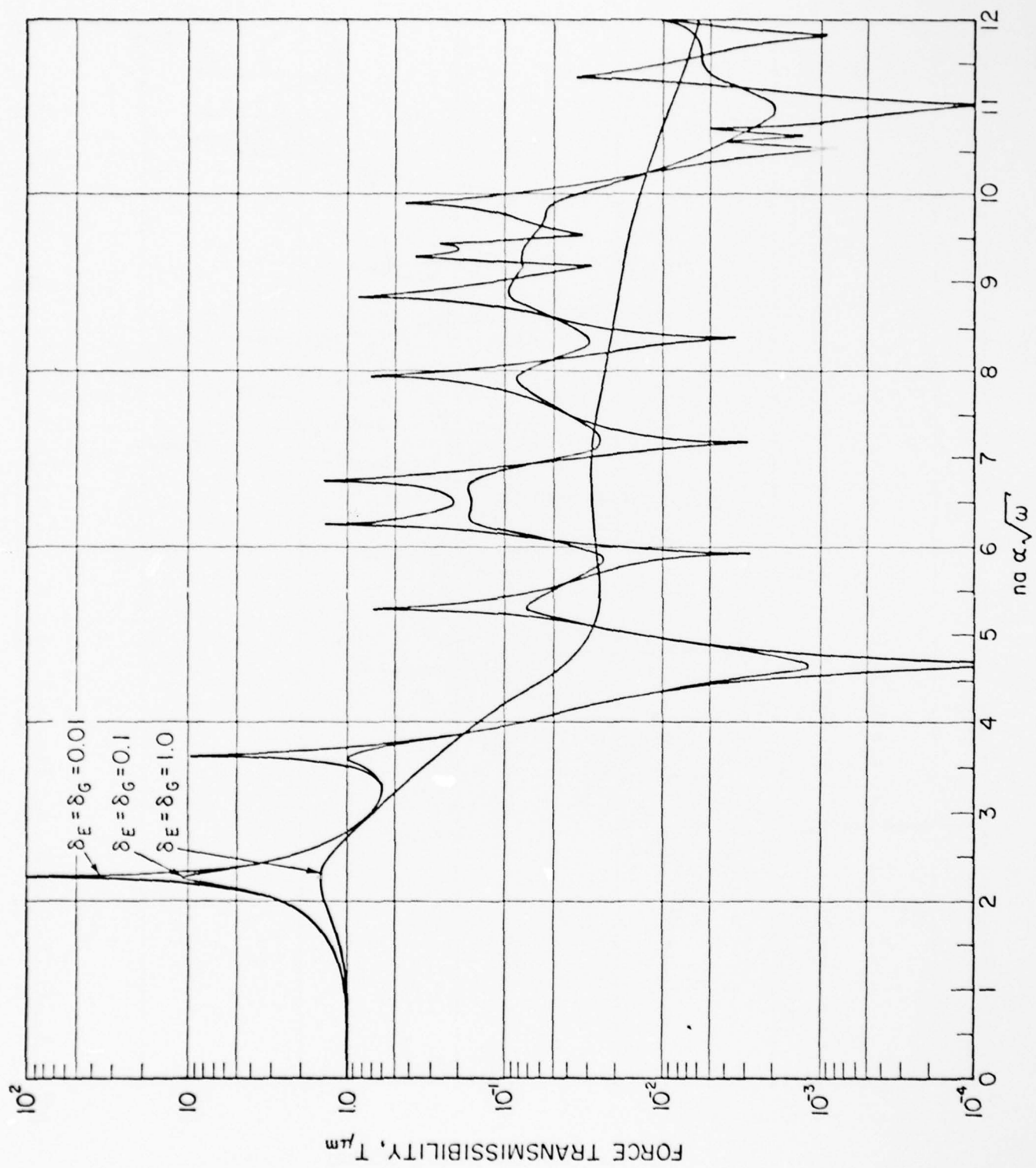


FIG. 13

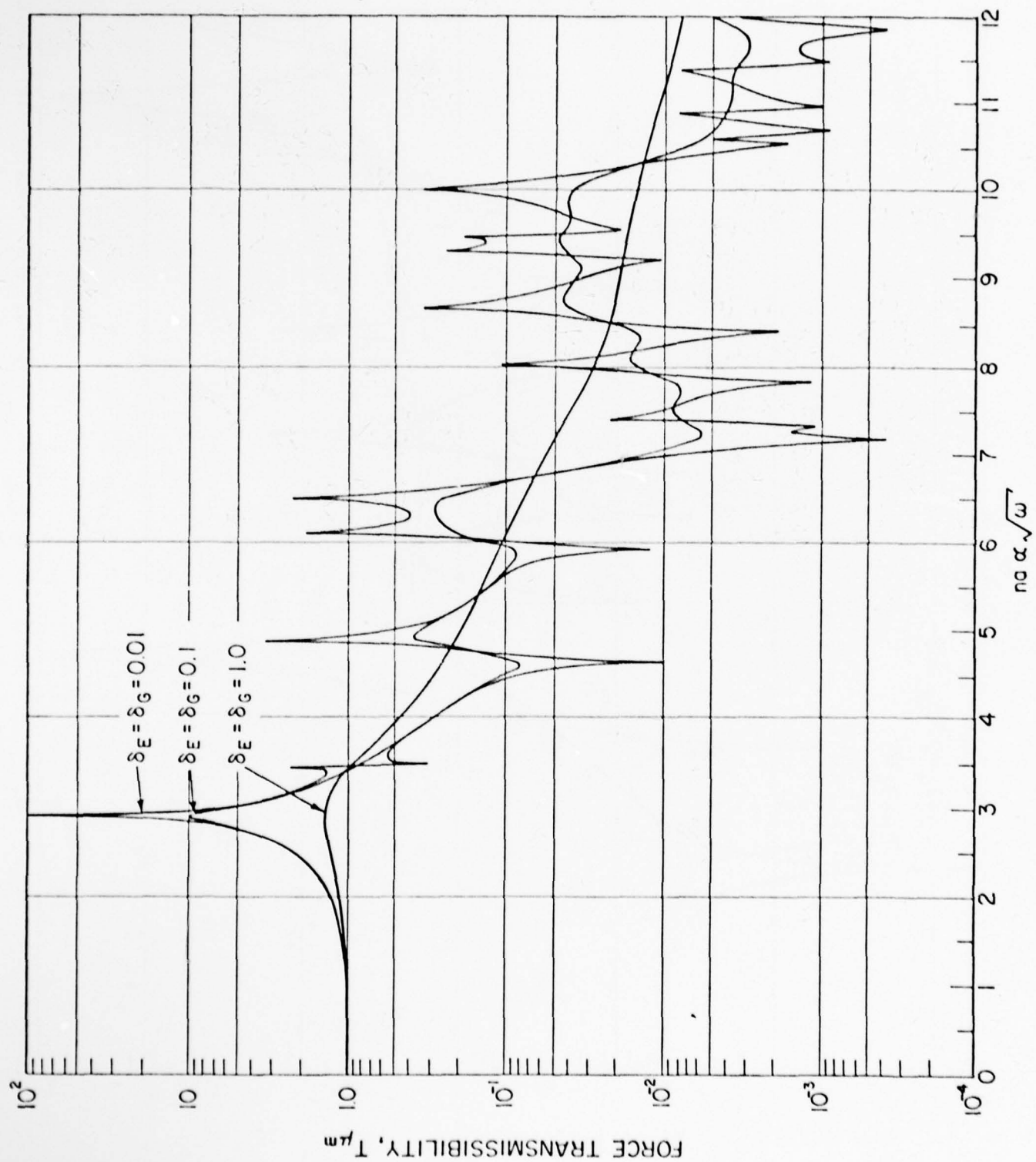


FIG. 14

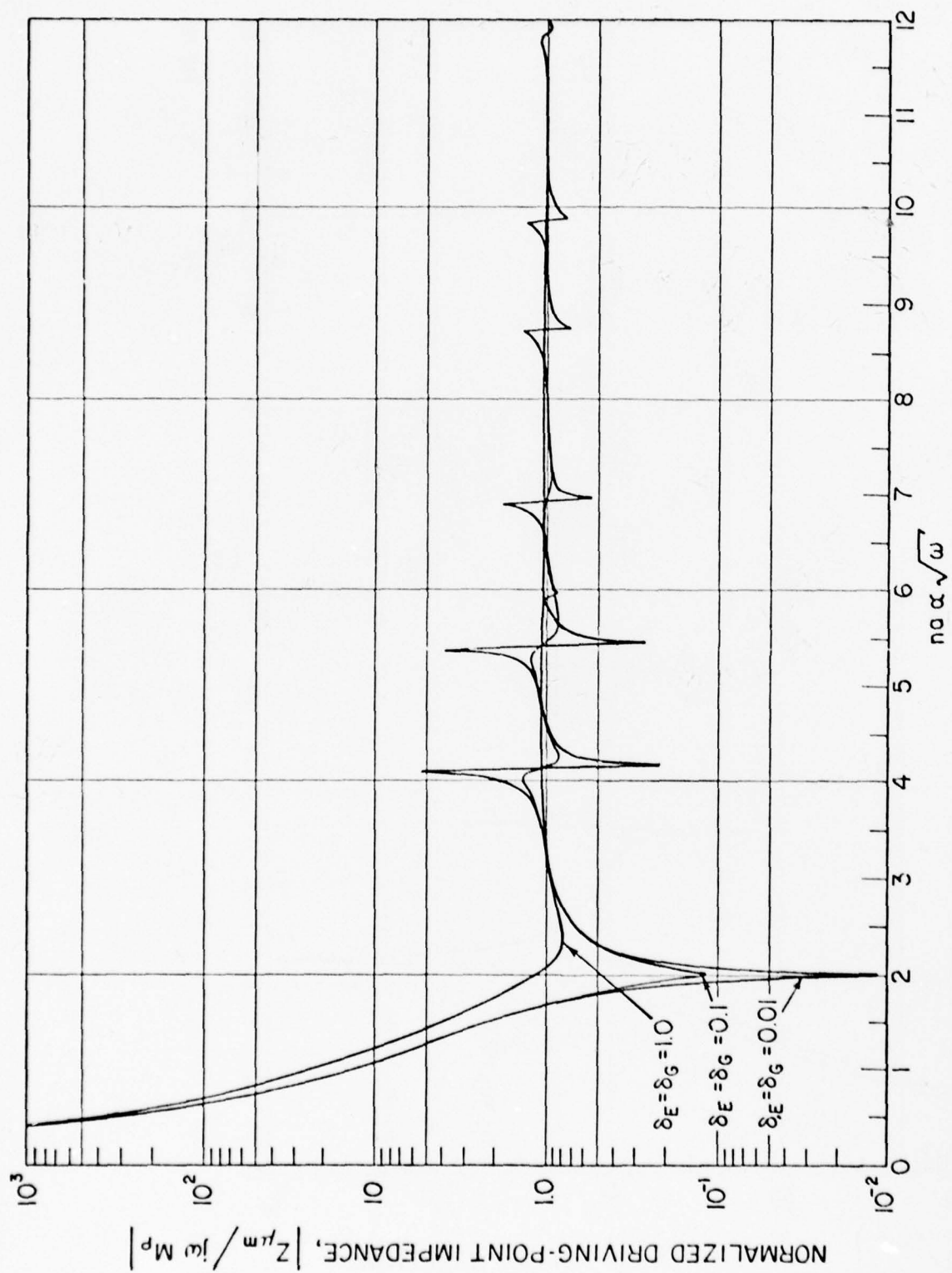


FIG. 15

FIG. 16

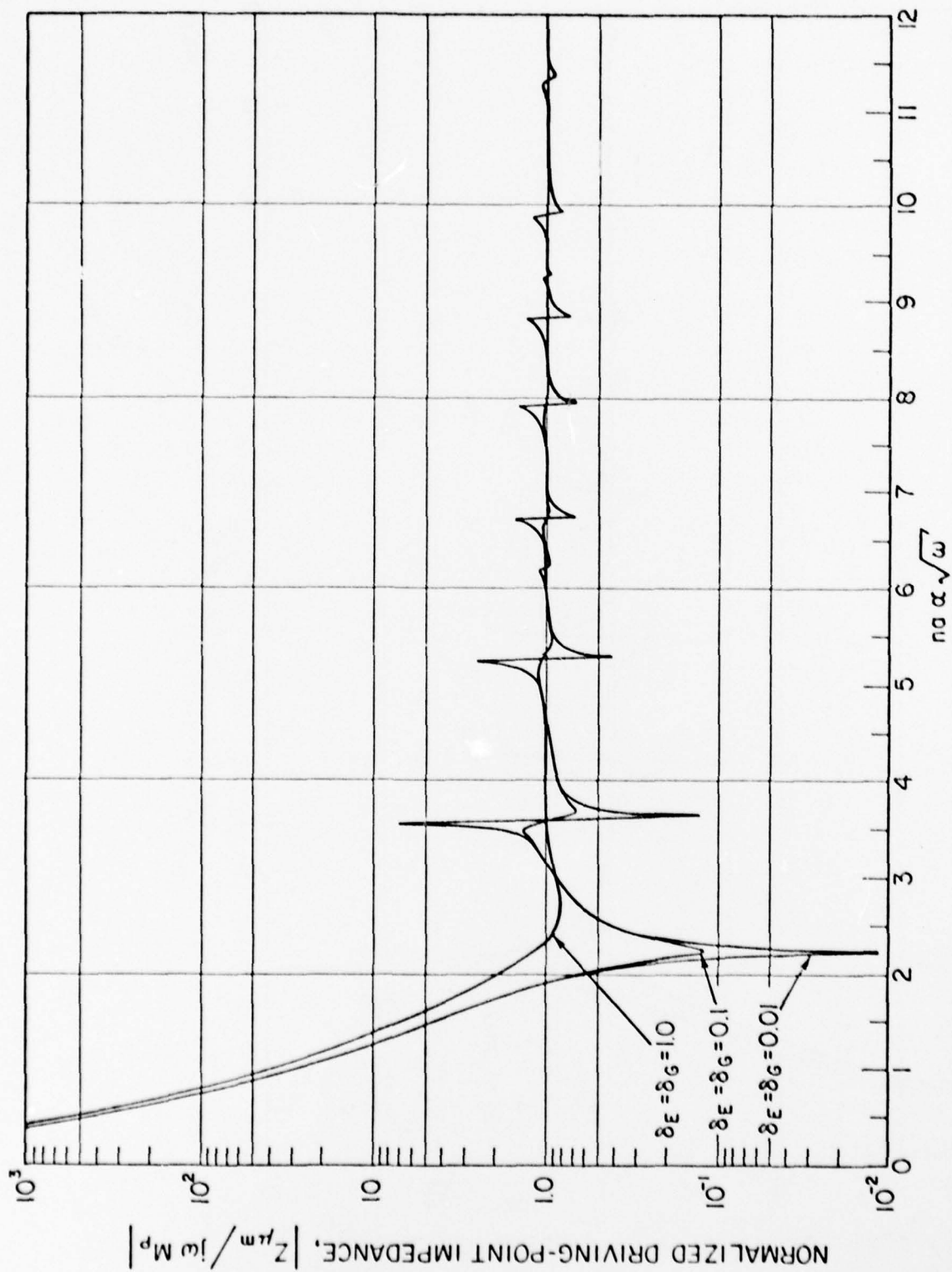
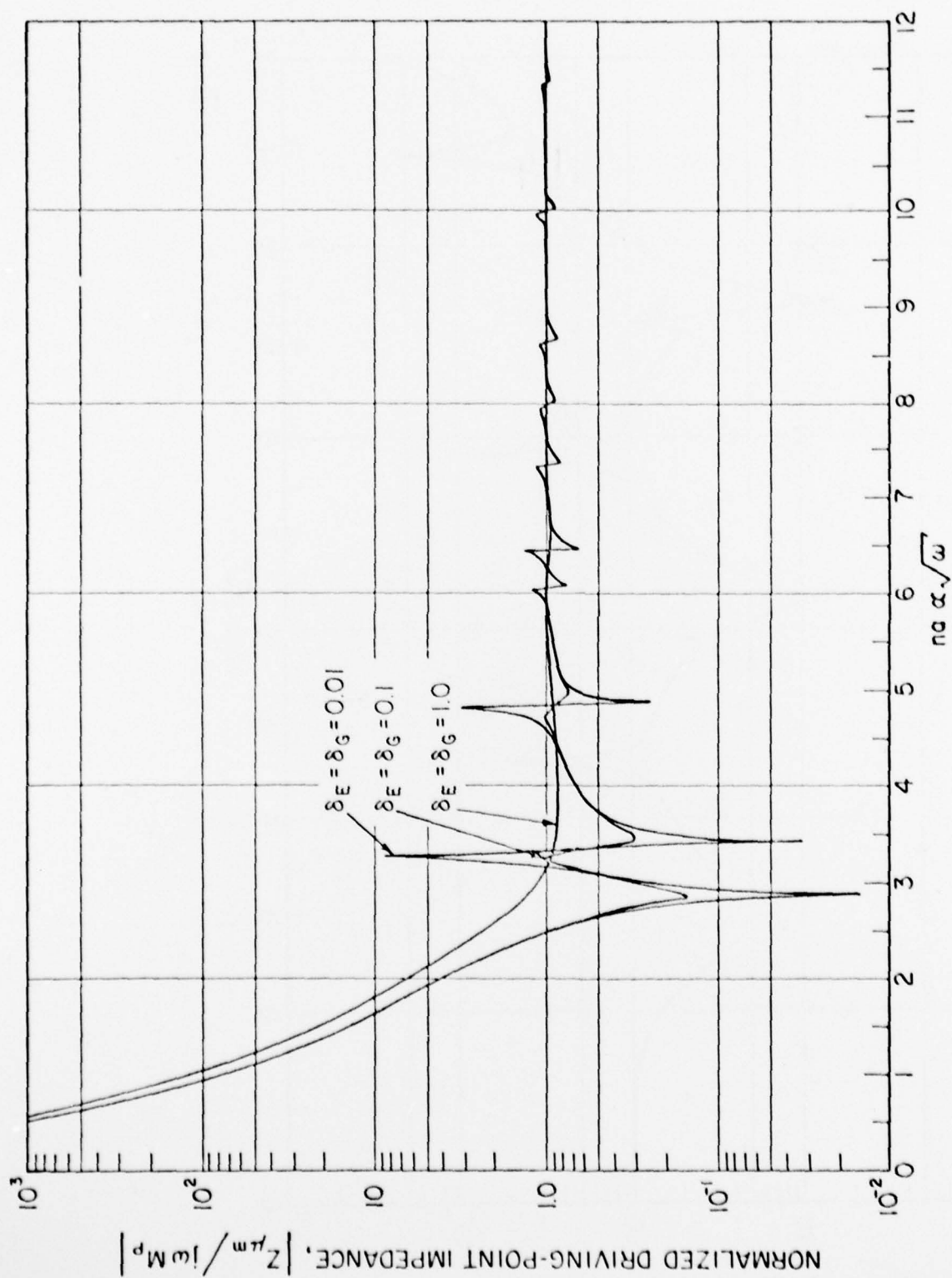




FIG. 17



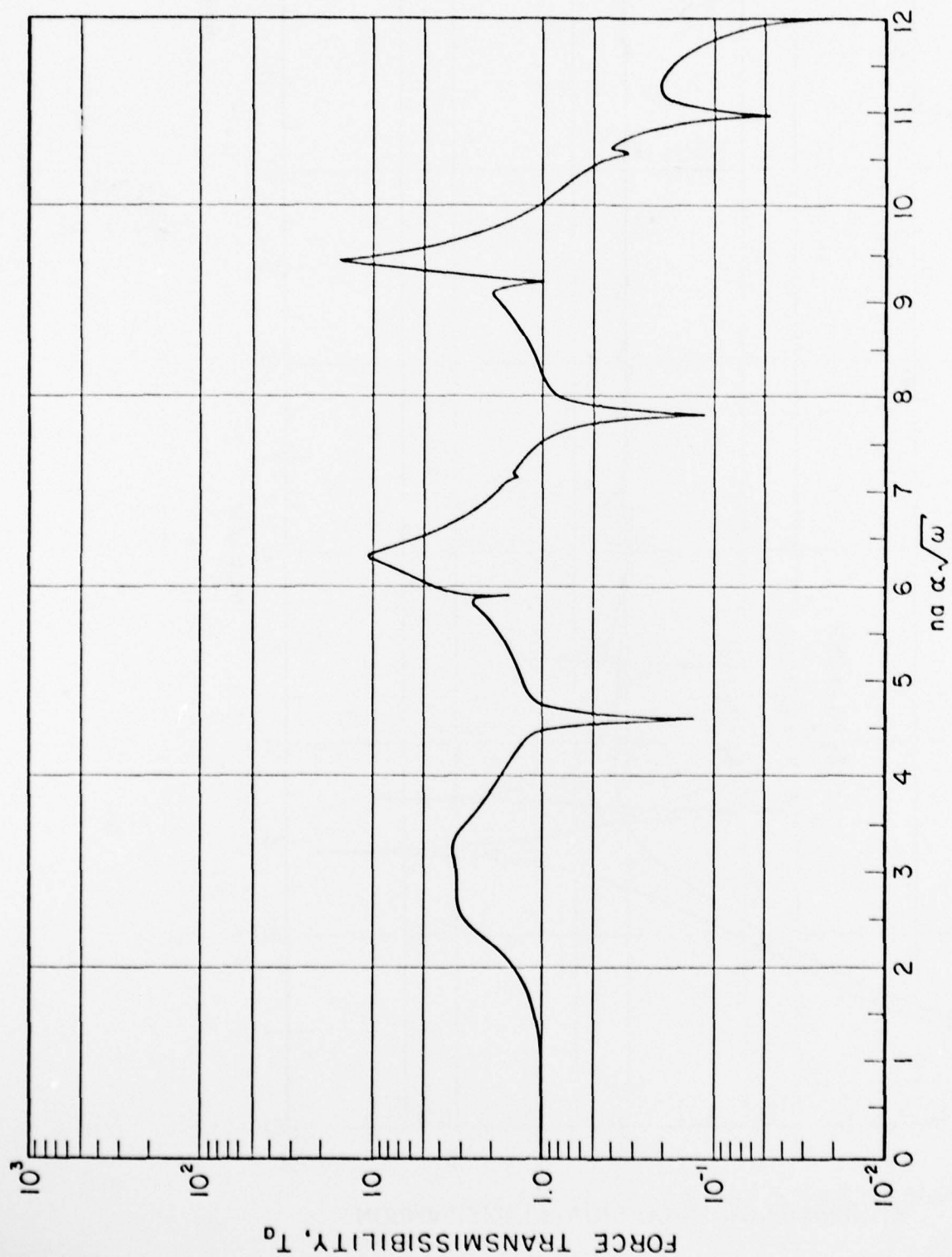
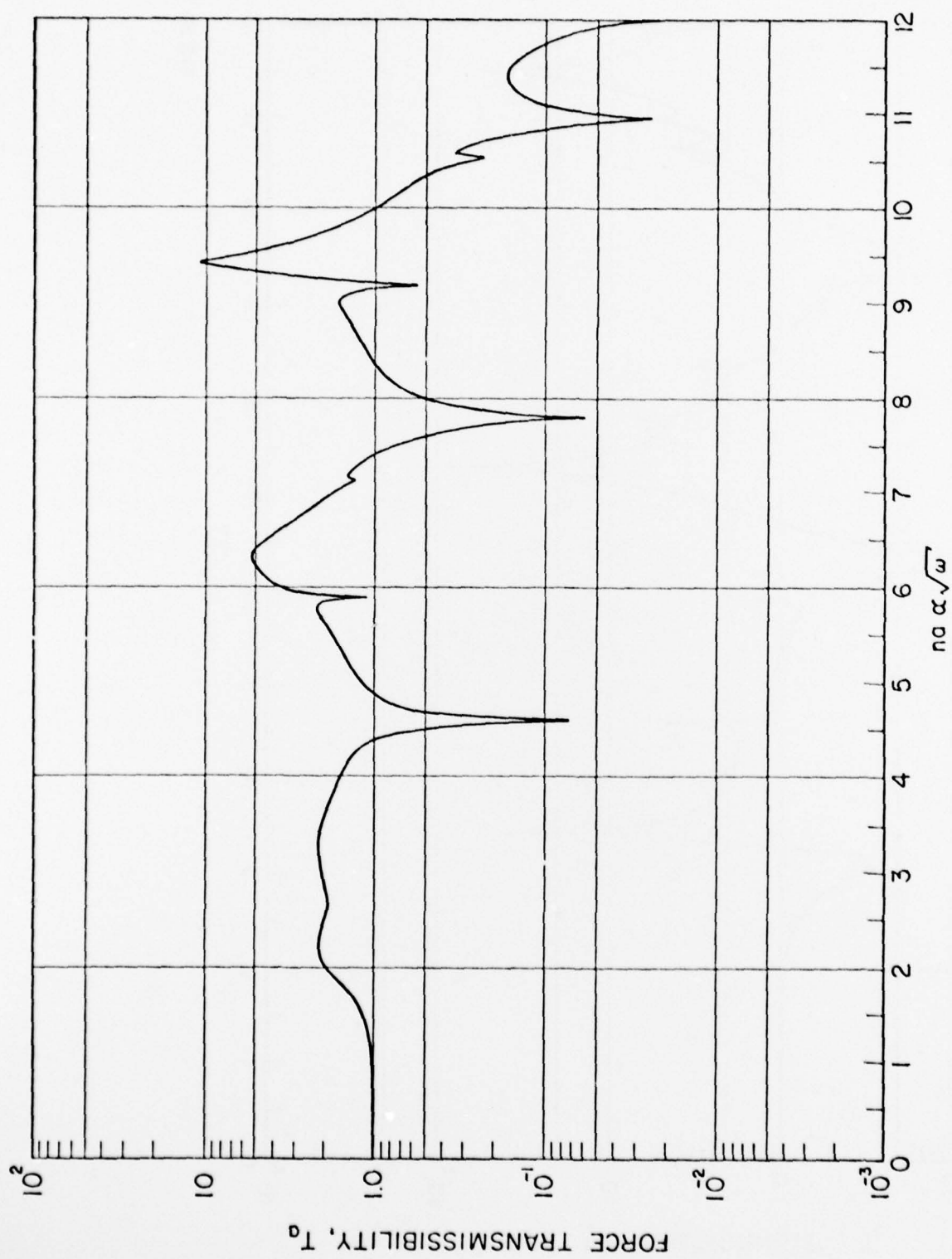


FIG. 19



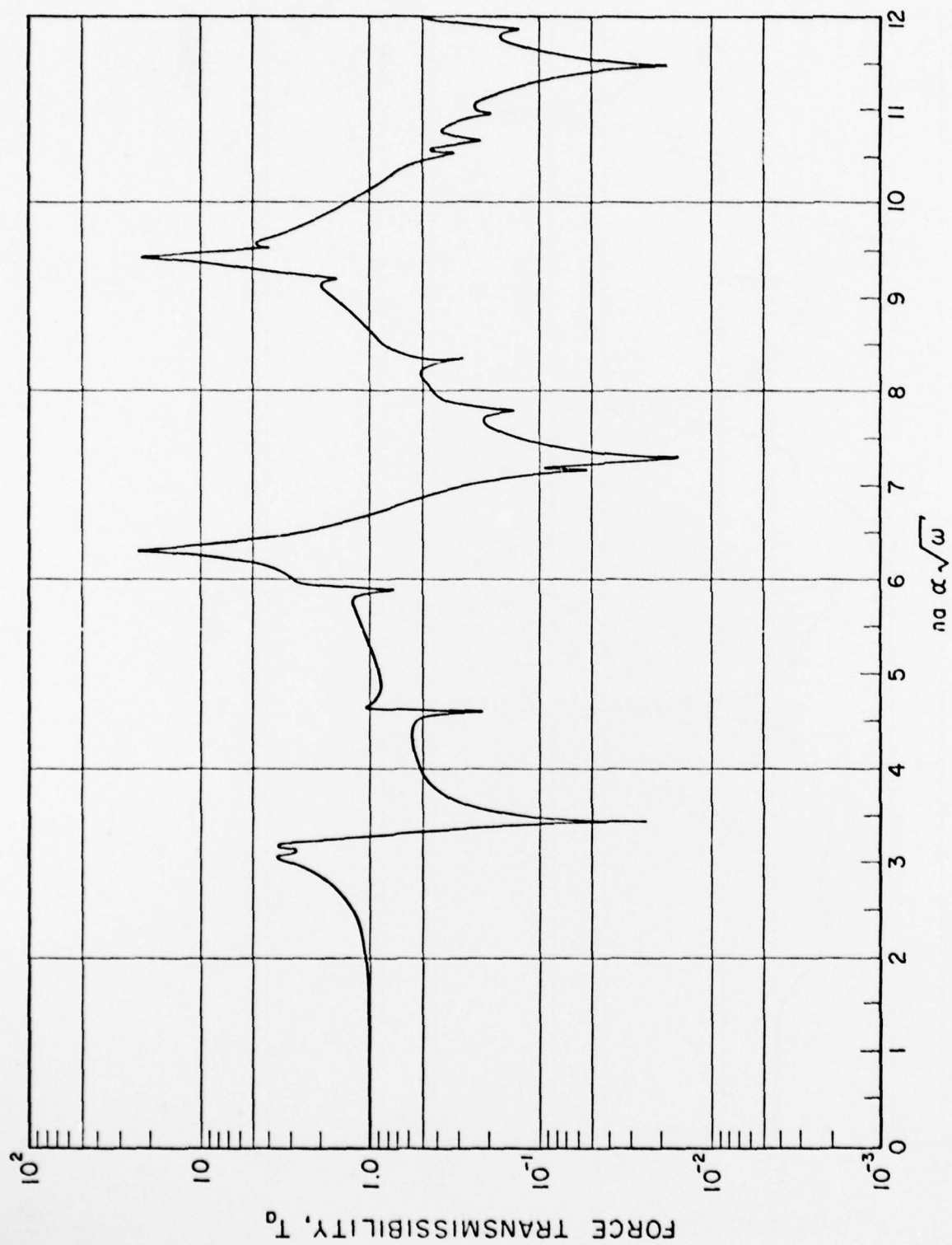


FIG. 20

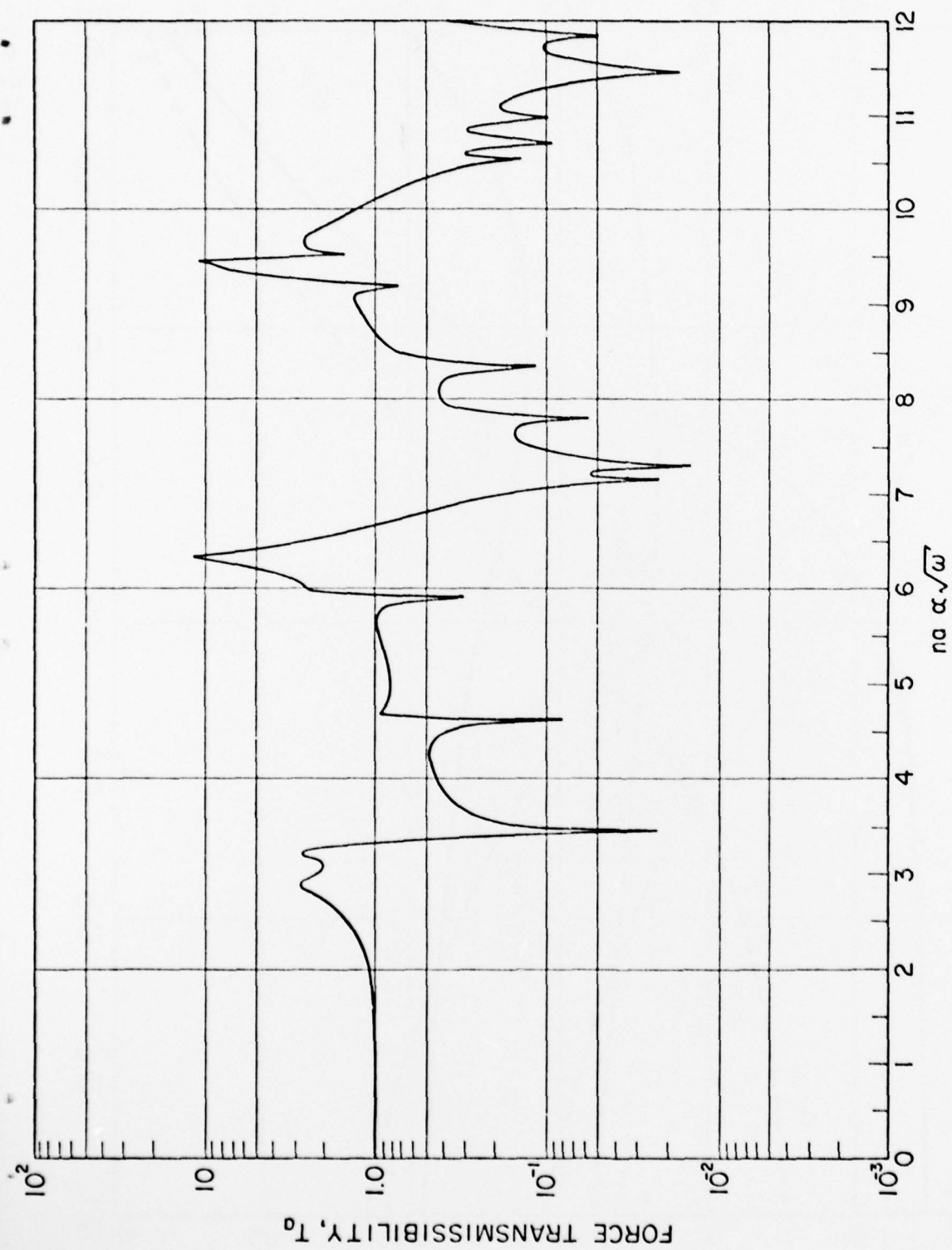


FIG. 21



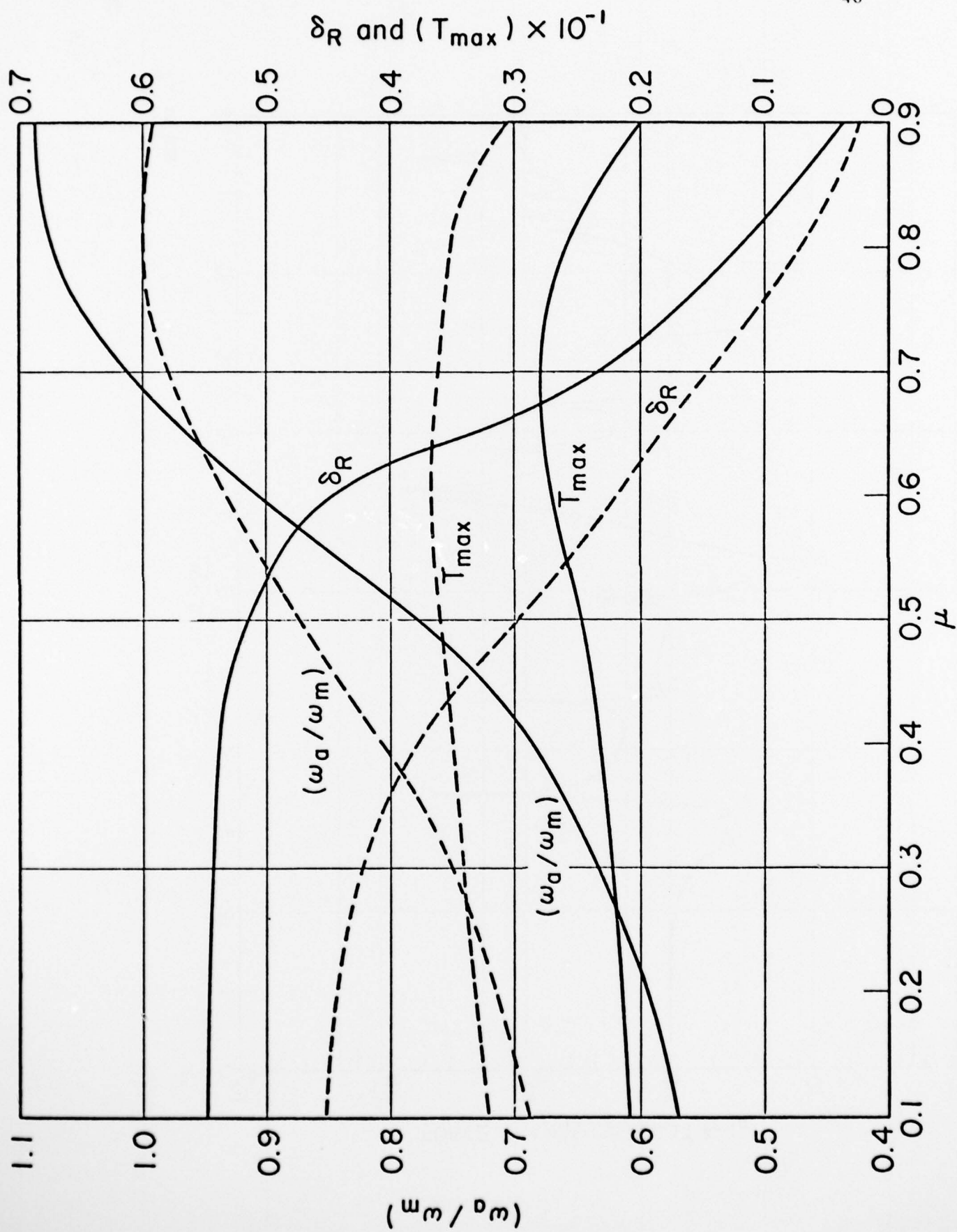
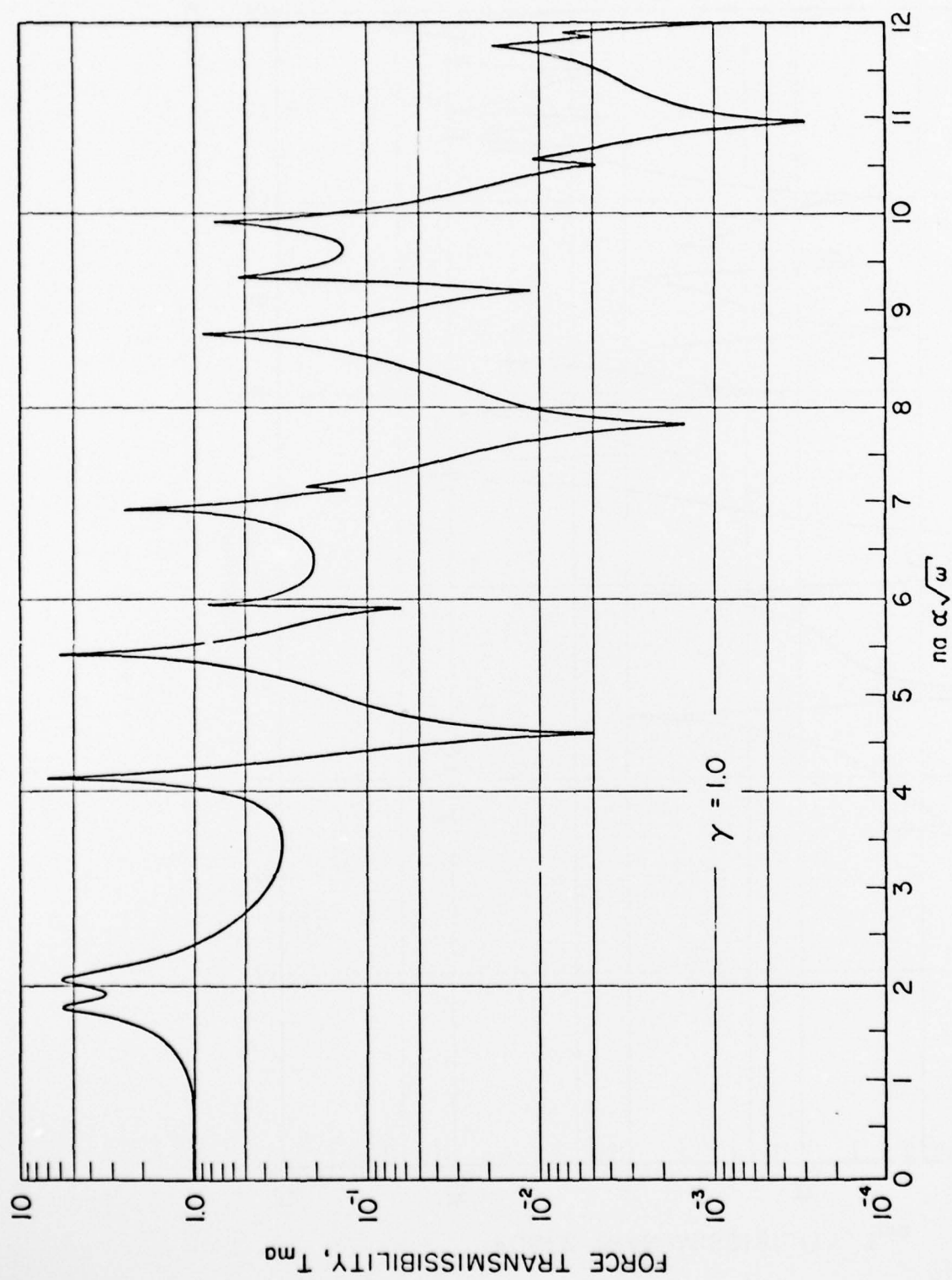


FIG. 22



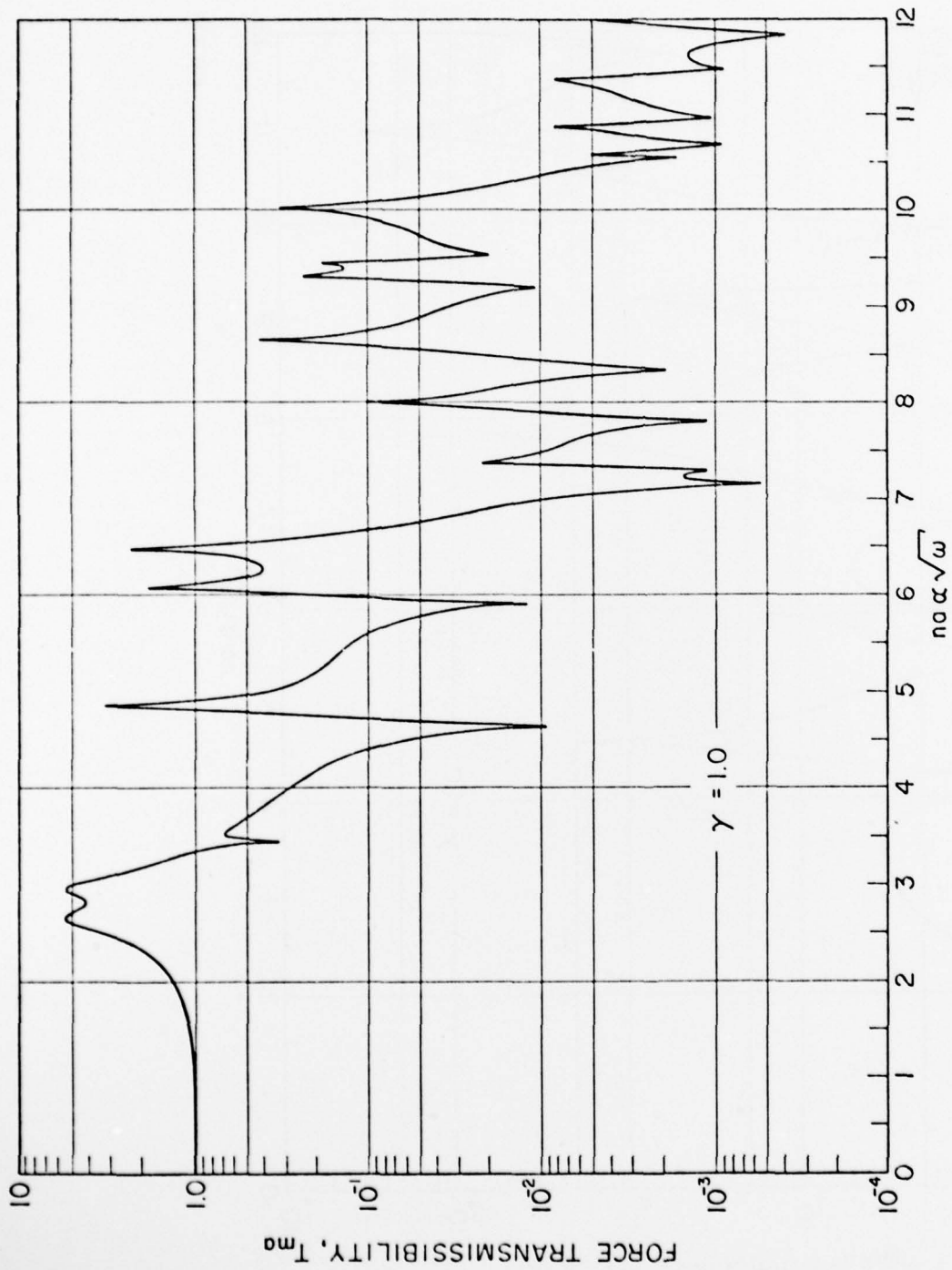


FIG. 24

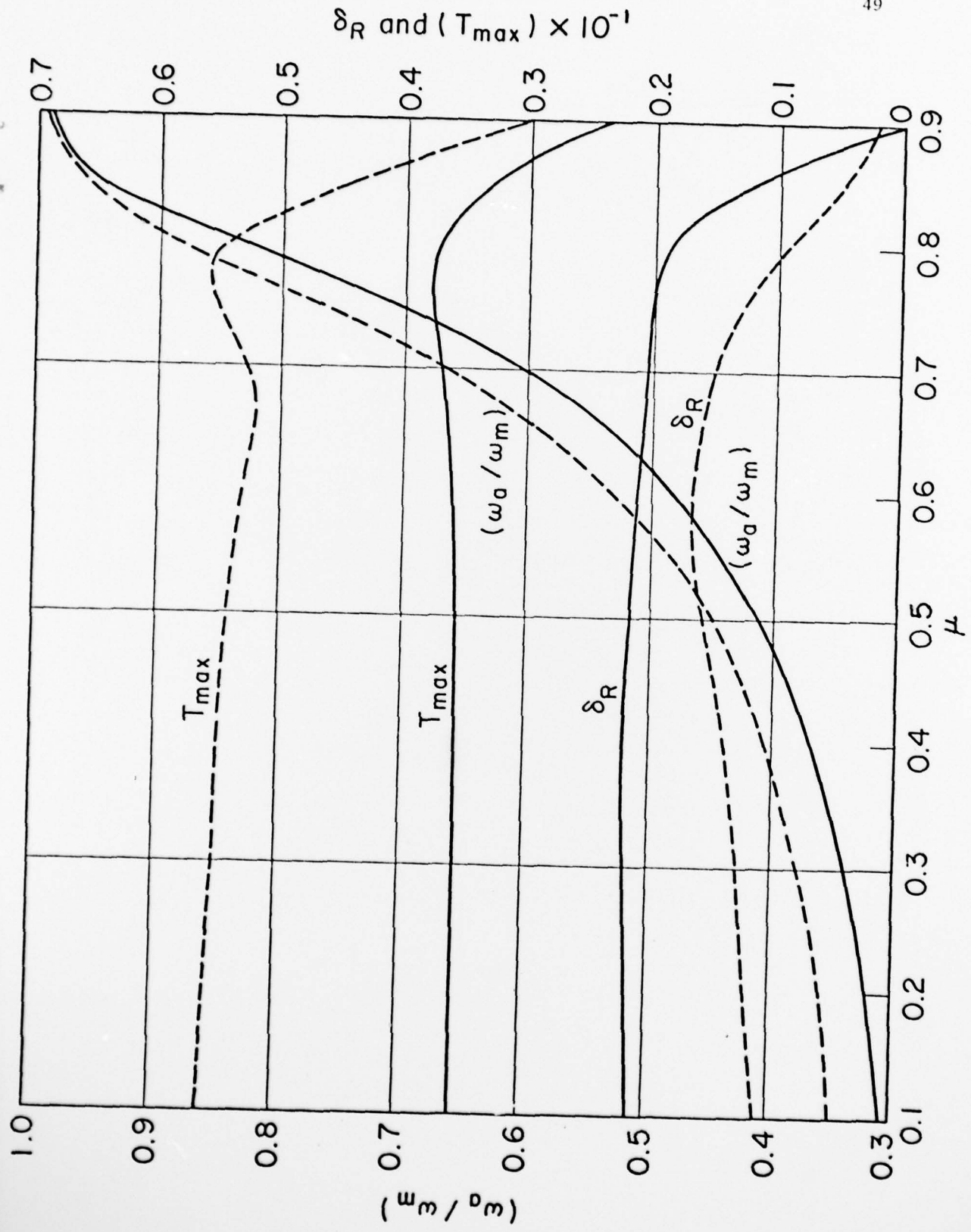


FIG. 25

DISTRIBUTION LIST FOR UNCLASSIFIED TM 79-191

1

Commander  
Naval Sea Systems Command  
Department of the Navy  
Washington, D.C. 20362  
Attn: Mr. Stephen M. Blazek  
SEA 05HB  
(Copy Nos. 1,2,3,4)

Commander  
Naval Sea Systems Command  
Department of the Navy  
Washington, D.C. 20362  
Attn: Mr. C. C. Taylor  
SEA 05H3  
(Copy Nos. 5 and 6)

Commander  
Naval Sea Systems Command  
Department of the Navy  
Washington, D.C. 20362  
Attn: SEA 921N  
(Copy No. 7)

Commander  
Naval Sea Systems Command  
Department of the Navy  
Washington, D.C. 20362  
Attn: PMS 393  
(Copy No. 8)

Commander  
Naval Sea Systems Command  
Department of the Navy  
Washington, D.C. 20362  
Attn: PMS 395  
(Copy No. 9)

Commander  
Naval Sea Systems Command  
Department of the Navy  
Washington, D.C. 20362  
Attn: PMS 396  
(Copy No. 10)

Commander  
Naval Sea Systems Command  
Department of the Navy  
Washington, D.C. 20362  
Attn: SEA 6103  
(Copy Nos. 11 and 12)

Commander  
Naval Sea Systems Command  
Department of the Navy  
Washington, D.C. 20362  
Attn: SEA 322  
(Copy No. 13)

Commander  
Naval Sea Systems Command  
Department of the Navy  
Washington, D.C. 20362  
Attn: SEA 3221  
(Copy No. 14)

Commander  
Naval Sea Systems Command  
Department of the Navy  
Washington, D.C. 20362  
Attn: SEA 3222  
(Copy No. 15)

Commander  
Naval Sea Systems Command  
Department of the Navy  
Washington, D.C. 20362  
Attn: SEA 6111  
(Copy Nos. 16 and 17)

Commander  
Naval Sea Systems Command  
Department of the Navy  
Washington, D.C. 20362  
Attn: SEA 6113  
(Copy Nos. 18 and 19)

Commander  
Naval Sea Systems Command  
Department of the Navy  
Washington, D.C. 20362  
Attn: SEA 6120  
(Copy Nos. 20 and 21)

Commander  
Naval Sea Systems Command  
Department of the Navy  
Washington, D.C. 20362  
Attn: SEA 3232  
(Copy No. 22)

Officer in Charge  
David W. Taylor Naval Ship  
Research and Development Center  
Annapolis Laboratory  
Annapolis, MD 21402  
Attn: Mr. J. Smith  
(Copy No. 23)

Officer in Charge  
David W. Taylor Naval Ship  
Research and Development Center  
Annapolis Laboratory  
Annapolis, MD 21402  
Attn: Mr. L. J. Argiro  
(Copy Nos. 24, 25, 26, 26, 28, 29)



Commander  
David W. Taylor Naval Ship Research  
and Development Center  
Bethesda, MD 20084  
Attn: Dr. M. Sevik  
(Copy Nos. 30 and 31)

Commander  
David W. Taylor Naval Ship Research  
and Development Center  
Bethesda, MD 20084  
Attn: Dr. W. W. Murray  
(Copy Nos. 32 and 33)

Commander  
David W. Taylor Naval Ship Research  
and Development Center  
Bethesda, MD 20084  
Attn: Dr. M. Strasberg  
(Copy No. 34)

Commander  
David W. Taylor Naval Ship Research  
and Development Center  
Bethesda, MD 20084  
Attn: Dr. G. Maidanik  
(Copy No. 35)

Commander  
David W. Taylor Naval Ship Research  
and Development Center  
Bethesda, MD 20084  
Attn: Dr. G. Chertock  
(Copy No. 36)

Commander  
David W. Taylor Naval Ship Research  
and Development Center  
Bethesda, MD 20084  
Attn: Dr. D. Feit  
(Copy Nos. 37, 38, 39, 40, 41, 42)

Commander  
David W. Taylor Naval Ship Research  
and Development Center  
Bethesda, MD 20084  
Attn: Mr. J. T. Shen  
(Copy No. 43)

Director  
Defense Documentation Center  
Cameron Station  
Alexandria, VA 22314  
(Copy Nos. 44, 45, 46, 47, 48, 49,  
50, 51, 52, 53, 54, 55)

Director  
Naval Research Laboratory  
Washington, D.C. 20390  
Attn. Code 8440  
(Copy Nos. 56 and 57)

Ocean Structures Branch  
U.S. Naval Research Laboratory  
Washington, D.C. 20390  
Attn: Mr. G. J. O'Hara  
(Copy No. 58)

Office of Naval Research  
Department of the Navy  
Arlington, VA 22217  
Attn: Dr. G. Boyer  
(Copy No. 59, 60, 61)

Office of Naval Research  
Department of the Navy  
Arlington, VA 22217  
Attn: Dr. A. O. Sykes  
(Copy Nos. 62, 63, 64)

Office of Naval Research  
Department of the Navy  
Arlington, VA 22217  
Attn: Mr. Keith M. Ellingsworth  
(Copy No. 65)

Office of Naval Research  
Department of the Navy  
Arlington, VA 22217  
Attn: Dr. N. Perrone  
(Copy NO. 66)

Commander  
Mare Island Naval Shipyard  
Vallejo, CA 94592  
(Design Division)  
(Copy No. 67)

Commander  
Portsmouth Naval Shipyard  
Portsmouth, NH 03801  
(Copy No. 68)

Supervisor of Shipbuilding,  
Conversion and Repair  
General Dynamics Corporation  
Electric Boat Division  
Groton, CT 06340  
Attn: Mr. John Wilder  
Dept. 440  
(Copy Nos. 69 and 70)

Supervisor of Shipbuilding,  
Conversion and Repair  
Ingalls Shipbuilding Corporation  
Pascagoula, MS 39567  
(Copy No. 71)

Supervisor of Shipbuilding,  
Conversion and Repair  
Newport News Shipbuilding  
Newport News, VA 23607  
(Copy No. 72)

Naval Ship Research and Development  
Center  
Underwater Explosion Research  
Division  
Portsmouth, VA 23709  
(Copy No. 73)

Commander  
Naval Underwater Systems Center  
New London Laboratory  
New London, CT 06320  
Attn: Mr. G. F. Carey  
(Copy No. 74)

Commander  
Naval Underwater Systems Center  
New London Laboratory  
New London, CT 06320  
Attn: Dr. R. S. Woollett  
(Copy No. 75)

Commander  
Naval Ocean Systems Center  
San Diego, CA 92052  
Attn: Library  
(Copy No. 76)

Dr. J. Barger  
Bolt Beranek and Newman, Inc.  
50 Moulton Street  
Cambridge, MA 02138  
(Copy No. 77)

Dr. D. I. G. Jones  
Air Force Materials Laboratory  
Wright-Patterson Air Force Base  
Ohio 45433  
(Copy No. 78)

Dr. M. C. Junger, President  
Cambridge Acoustical Associates, Inc.  
54 Rindge Avenue  
Cambridge, MA 02140  
(Copy No. 79)

Acquisitions Supervisor  
Technical Information Service  
American Institute of Aeronautics  
and Astronautics, Inc.  
750 Third Avenue  
New York, NY 10017  
(Copy No. 80)

Dr. R. S. Ayre  
Department of Civil Engineering  
University of Colorado  
Boulder, CO 80302  
(Copy No. 81)

Dr. D. Frederick  
Chairman, Engineering Science and  
Mechanics Department  
Virginia Polytechnic Institute  
and State University  
Blacksburg, VA 24061  
(Copy No. 82)

Dr. D. E. Hudson  
Department of Mechanics  
California Institute of Technology  
Pasadena, CA 91109  
(Copy No. 83)

Dr. G. Herrman, Chairman  
Department of Applied Mechanics  
Stanford University  
Stanford, CA 94305  
(Copy No. 84)

Dr. A. Kalnins  
Department of Mechanical Engineering  
and Mechanics  
Lehigh University  
Bethlehem, PA 18015  
(Copy No. 85)

Dr. Y. H. Pao, Chairman  
Department of Theoretical and  
Applied Mechanics  
Cornell University  
Ithaca, NY 14850  
(Copy No. 86)

Dr. D. D. Kana  
Southwest Research Institute  
8500 Culebra Road  
San Antonio, TX 78206  
(Copy No. 87)

Dr. J. R. Rice  
School of Engineering  
Brown University  
Providence, RI 02912  
(Copy No. 88)

Dr. P. S. Symonds  
School of Engineering  
Brown University  
Providence, RI 02912  
(Copy No. 89)

Dr. W. J. Worley  
Department of Theoretical and  
Applied Mechanics  
University of Illinois  
Urbana, IL 61801  
(Copy No. 90)

Dr. Dana Young  
Southwest Research Institute  
8500 Culebra Road  
San Antonio, TX 78206  
(Copy No. 91)

Dr. R. M. Gorman  
Bolt Beranek and Newman, Inc.  
Union Station  
New London, CT 06340  
(Copy No. 92)

Commander  
Naval Sea Systems Command  
Department of the Navy  
Washington, D.C. 20362  
Attn: SEA 9661-Library  
(Copy No. 93 and 94)